Report No. ACNP - 64016

PATHFINDER ATOMIC POWER PLANT

BOILER FUEL ELEMENT CONCEPTUAL DESIGN REPORT

Submitted to

U. S. ATOMIC ENERGY COMMISSION

NORTHERN STATES POWER COMPANY

and

CENTRAL UTILITIES ATOMIC POWER ASSOCIATES

by

ALLIS-CHALMERS MANUFACTURING COMPANY
ATOMIC ENERGY DIVISION
Milwaukee 1, Wisconsin

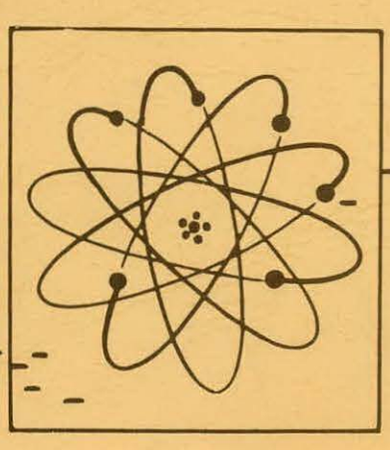

Ref: AEC Contract No. AT(11-1)-589

DISCLAIMER

LEGAL NOTICE

This report was prepared as an account of Government sponsored work. Neither the United States, nor the Commission, nor Allis-Chalmers Manufacturing Company, nor any person acting on behalf of the Commission or Allis-Chalmers Manufacturing Company:

A. Makes any warranty or representation to others, expressed or implied, with respect to the accuracy, completeness, or usefulness of the information contained in this report, or that the use of any information, apparatus, method, or process disclosed in this report may not infringe privately owned rights; or

B. Assumes any liabilities to others with respect to the use of, or for damages resulting from the use of any information, apparatus, method, or process disclosed in this report.

As used in the above, 'person acting on behalf of the Commission or Allis-Chalmers Manufacturing Company' includes any employe or contractor of the Commission, or Allis-Chalmers Manufacturing Company or employe of such contractor, to the extent that such employe or contractor of the Commission, or Allis-Chalmers Manufacturing Company or employe of such contractor prepares, disseminates, or provides access to, any information pursuant to his employment or contract with the Commission or Allis-Chalmers Manufacturing Company or his employment with such contractor.

PATHFINDER ATOMIC POWER PLANT

BOILER FUEL ELEMENT DESIGN REPORT

By D. A. Patterson, W. J. Severson,
D. R. Roberts and R. H. Klumb

Submitted to

U. S. ATOMIC ENERGY COMMISSION
NORTHERN STATES POWER COMPANY
and
CENTRAL UTILITIES ATOMIC POWER ASSOCIATES
by
ALLIS-CHALMERS MANUFACTURING COMPANY

Under
Agreement dated 2nd Day of May 1957, as Amended
between
Allis-Chalmers Mfg. Co. & Northern States Power Co.
under
AEC Contract No. AT(11-1)-589

January 8, 1965

Classification – UNCLASSIFIED

Approved: C. B. Graham

C. B. Graham
General Manager's Staff

ALLIS-CHALMERS MANUFACTURING COMPANY
ATOMIC ENERGY DIVISION
BETHESDA, MD. 20014

Approved: Hibbert Hill

Hibbert Hill
Vice President-
Engineering

NORTHERN STATES POWER COMPANY
15 SOUTH FIFTH STREET
MINNEAPOLIS 2, MINNESOTA

PATHFINDER ATOMIC POWER PLANT

BOILER FUEL ELEMENT DESIGN REPORT

DISTRIBUTION

USAEC, Chicago Operations Office -- 9800 South Cass Avenue, Argonne, Illinois	5
USAEC, Division of Reactor Development -- Washington 25, D. C.	8
USAEC, OTIE -- Oak Ridge, Tennessee ... OFFSET MASTER PLUS	20
Northern States Power Company and CUAPA	26
Allis-Chalmers Manufacturing Company	39
Total	98

FOREWORD

One of a series of reports on research and development in connection with the design of the Pathfinder Atomic Power Plant, this particular report deals with Boiler Fuel Element Design. The Pathfinder Plant is located at a site near Sioux Falls, South Dakota and reached criticality early in 1964. Owners and operators of the plant will be Northern States Power Company of Minneapolis, Minnesota. Allis-Chalmers is performing the research, development and design, as well as being responsible for plant construction.

The U. S. Atomic Energy Commission, through Contract No. AT(11-1)-589 with Northern States Power Company, and Central Utilities Atomic Power Associates (CUAPA) are sponsors of the research and development program. The plant's reactor will be of the Controlled Recirculation Boiling Reactor type with Nuclear Superheater.

CONTENTS

CONTENTS - (Continued)

LIST OF ILLUSTRATIONS

LIST OF ILLUSTRATIONS

1.0 INTRODUCTION

This report describes the mechanical design of the boiler fuel element assemblies comprising the first boiler core of the Pathfinder Reactor. The nuclear and heat transfer design and expected performance of these fuel elements are covered in other reports. The following data are presented for the purpose of describing the operating conditions, fuel loading, expected life and as a basis for the assumptions made in the following sections of this report:

Core

Mean equivalent outside diameter	in	69.0
Mean equivalent inside diameter	in	31.3
Active fuel length	in	72
Volume	ft^3	123
No. of fuel element assemblies		96
Average power density	KW/FT^3 core volume	1280
Average specific power	KW/Kg of Uranium	24.0
Average heat flux	$Btu/hr/ft^2$	122,000
Maximum heat flux	$Btu/hr/ft^2$	447,000
Burnout heat flux	$Btu/hr/ft^2$	1,080,000
Maximum fuel temp.	^oF	3860
Maximum Clad surface temp.	^oF	514
Inlet cooling velocity	Ft/sec	13.6
Exit voids	%	45.5
Pressure Drop (Max)	Psi	13.6
Fuel Burnup	MWD/T	10,000
Core lifetime	Yr	1.5
Fuel Enrichment U-235	w/o	2.2 & 3.2
Fuel Loading, U	Kg	6606

Fuel Element Assemblies

Fuel Material		UO_2
Fuel Density	gm/cc	10.41
Cladding material		Zirc-2
Nozzle material		Stainless Stl

Fuel Element Assemblies

Thermal Power Generated	MW	157.4
Heat Transfer Area	Ft^2	4397
Coolant Flow Area, Lower Half	Ft^2	9.43
Coolant Flow Area, Upper Half	Ft^2	10.81

2.0 CONCEPTUAL DESIGN

2.1 Criteria

In order to reduce radial power gradients and for mechanical reasons, the central superheater was made in a generally cylindrical shape. The boiler core was then located around the superheater in two annular regions containing eight control rods each. For adequate control rod cooling, each of the eight rods is guided in a fully contained channel. In the interest of reducing structural material, the control rod channel walls were made part of the fuel channels. This resulted in two types of fuel channels; the four channels clustered around the control rods, and those in the spaces left over. See Figure 1.

Preliminary pressure drop results indicated that the probable weight of the element was not enough to hold it down. This required a holddown scheme of some sort. It was decided to use a massive structure on top of the elements which also incorporated the above-core control rod guides and flow deflectors. The holddown structure rested on a stainless steel baffle surrounding the boiler core.

The use of a holddown defined a fixed axial area for the fuel elements and dictated that provision be made for differential expansion.

In view of Pathfinder's high power density, 46 kw/l, it was desirable to take advantage of localized fuel depletion to reduce within cell peak-to-average factors. This required some provision for selective orientation of the fuel element around a control rod channel (control rod followers were not used).

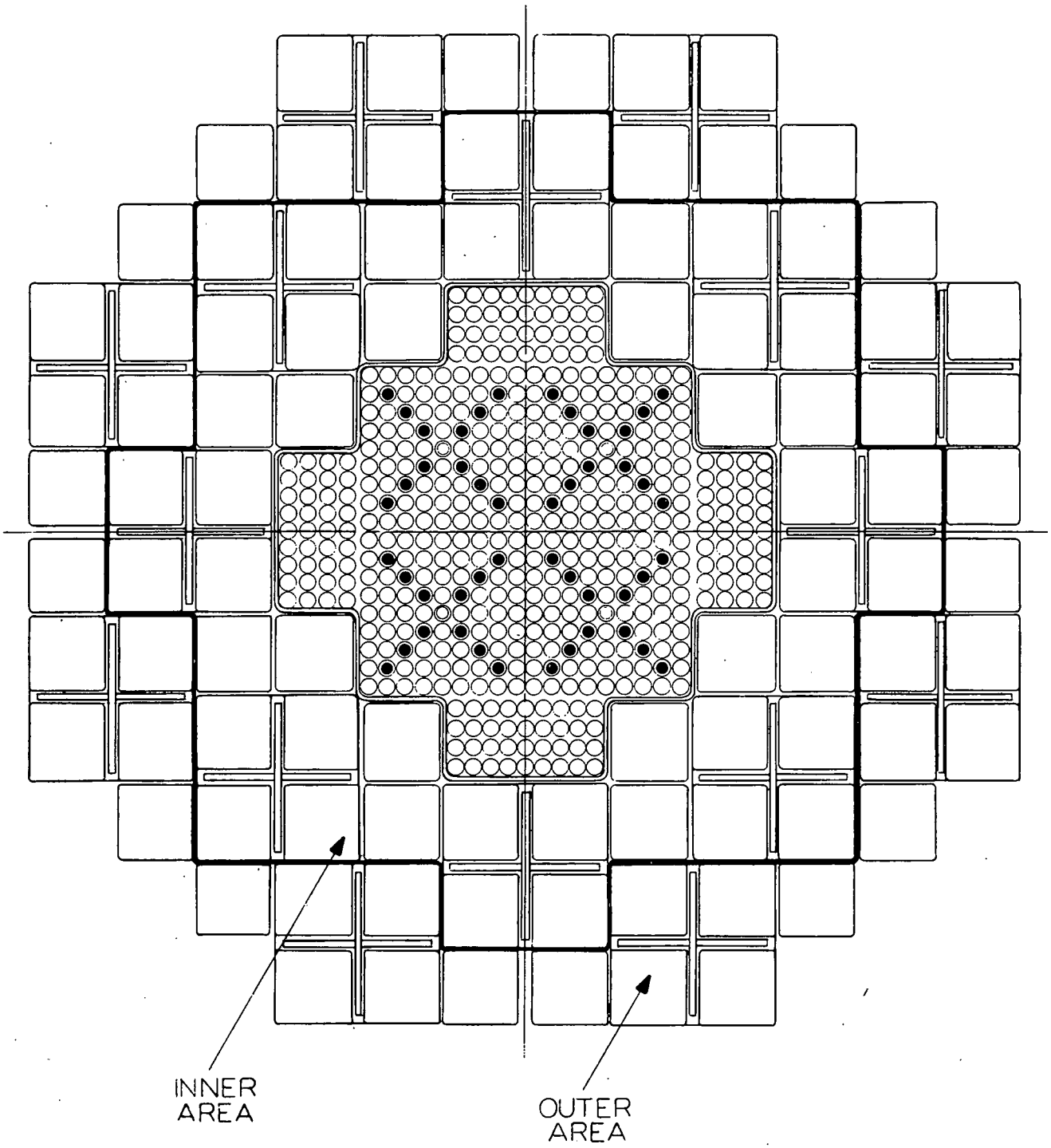

Figure 1...Plan View of Boiler and Superheater Cores

2.2 Philosophy

After establishing the criteria, the design philosophy for the boiler fuel element was established. Schedule and funds did not allow engineering from test and development results, but required that a design be established and sufficient testing done to substantiate the design. This dictated appreciable conservatism where data or experience were not available.

Mechanical assembly was selected in favor of welded and/or brazed construction. The conceptual fuel assembly consisted of a number of individual components, each of which could be inspected and accepted or rejected. These components were, in turn, to be assembled in such a fashion that any further operations would not alter them or jeopardize the partially assembled element. Further, it was decided to set tolerances and requirements which provide complete interchangeability of components. However, interchangeability was violated to some extent by the over-riding requirement for a prescribed orientation of the elements in the channels.

2.3 Design

The particular core arrangement required two types of Zircaloy fuel channels or boxes. The first (Quad Box) contains a control rod guide channel surrounded by four boiler elements. The second (Single Box) contains only one element.

The boxes are fabricated from Zircaloy and have stainless steel base plates fastened to the side walls with flat head machine screws.

The fuel element rests on the base plate, holding the box down to the grid plate. The element is, in turn, held down by the holddown structure.

The quad boxes contain a cruciform shaped plenum, which is fed from a coolant hole through the grid plate. The coolant flow then goes through a number of long, self-orificing holes into the control rod channel. The clearance between the box and fuel element was selected to provide adequate clearance for fuel insertion. Underwater fuel handling tests have proven the clearance adequate for easy insertion.

The fuel element is centered at each end. At the lower end, the nozzle ring centers (see Figure 3) the box and element in respect to the core grid plate. The upper end fitting has a nominal clearance of 0.050 in. between the box and itself. Differential thermal expansion will greatly decrease the clearance during operation, centering the fuel element at the top.

During operation, the clearance between the tube sheets and the box will be approximately .045 in. The flux peak from the resulting water gap was included in the hot spot factors.

Fretting corrosion at the point of contact between tube sheet skid and the box (when the element is off center at that elevation) is not expected because the element, experiencing a considerable compressive load (440 lb), will align itself against one side of the box and remain in that position. It is very unlikely that the element will vibrate as an assembly; i.e., the element will not oscillate from one side of the box to the other, especially since there are 81 rods all vibrating in different planes and at slightly different frequencies.

Selection of the water fuel ratios (top and bottom) was based on the usual considerations, but was further influenced by the presence of the integral superheater.

The heat flux at the outside surface of the fuel rod was limited by clad heat transfer burnout criteria. The established heat flux further dictated the number of fuel rods per assembly and the number of assemblies.

The fuel assemblies were designed to operate at average fuel rod specific powers of 24 kw/kg of uranium, for average burnups of 6600 MWD/ton and 10,000 MWD/ton for the single and quad box assemblies, respectively.

The stepped fuel rod concept was considered the most economical approach to compensate for moderator voiding in the upper half of the core, and to provide power flattening.

The active core length was specified to be 72 in. A vibrational analysis and experiments indicated that a 36 in. unsupported rod was marginal at best. (This test is discussed in Section 4.2). The stepped fuel rod concept lends itself very readily to a joint and spacer at the midpoint of the core. Accordingly, other spacers were located at the midpoints of the upper and lower core halves. The segmented rod (Figure 3) was chosen since it presented the most practical method of spacing and preventing lateral movement of the fuel rods. This resulted in a 9 x 9 array with each fuel rod axially segmented into four sections.

The power fraction of each fuel rod segment, core and cell radial hot spot factors, and axial power distribution were employed to describe the hottest fuel rod. The mechanical factors were assumed the same for all fuel rods.

Fuel elements located in the quad boxes are exposed to a more uneven cell radial flux distribution (because of the increased quantity of moderator in the control rod channel) than fuel elements located in the single boxes. The inside corner fuel rod of the quad box element, adjacent to the intersection of the cruciform channel is the worst rod from the standpoint of fission product buildup and temperature. See Figure 2. Table I shows the power distribution, radial hot spot factors, and temperature for each of the four fuel rod sections that make up the hot fuel rod. The temperatures computed were calculated excluding eccentricity of the pellet. The boiler core power is 157.4 MW with a maximum hot spot factor of 3.5.

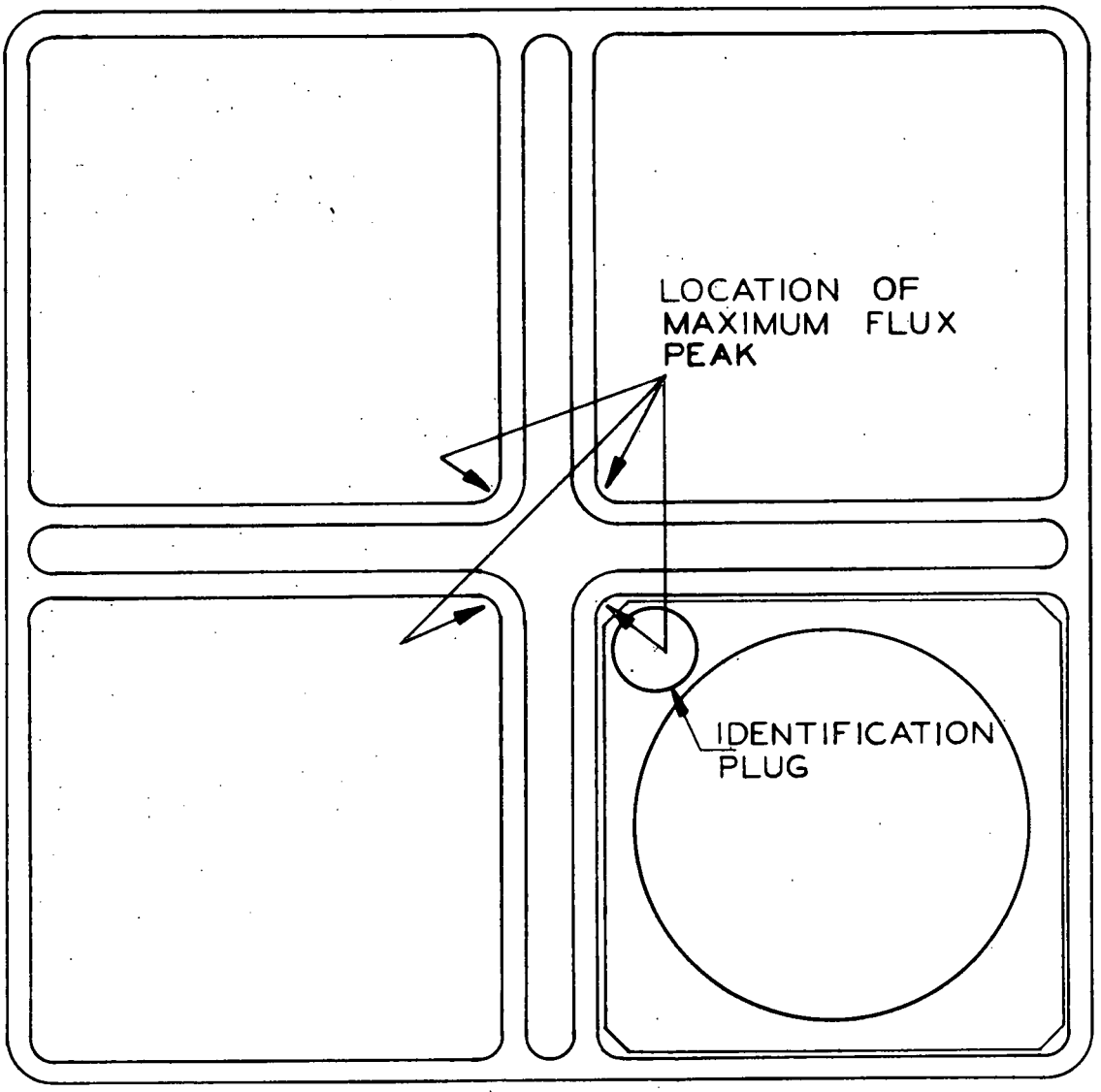

TOP VIEW OF QUAD BOX SHOWING
ORIENTATION OF FUEL ELEMENT

Figure 2...Top View of Quad Box Showing Orientation of Fuel Element (43-025-445)

TABLE I

CORE OPERATING PARAMETERS FOR HOTTEST ROD

	Rod I	Rod II	Rod III	Rod IV
Beginning of Life				
Power Fraction	36.7%	34.29%	19.35%	9.64%
Radial Hot Spot Factor	1.67	1.67	1.71	1.71
Pellet Temp. (centerline)	3860 F	3690 F	2409 F	1507 F
Pellet Temp. (mean)	2240 F	2155 F	1515 F	1064 F
Pellet Temp. (Surface)	620 F	620 F	---	---
Middle of Life				
Power Fraction	31.6%	32.65%	23.4%	12.36%
Radial Hot Spot Factor	1.56	1.56	1.54	1.54
Pellet Temp. (centerline)	3226 F	3345 F	2568 F	1644 F
Pellet Temp. (mean)	1923 F	1983 F	1594 F	1132 F
End of Life				
Power Fraction	26.48%	31.01%	27.44%	15.07%
Radial Hot Spot Factor	1.46	1.46	1.37	1.37
Pellet Temp. (centerline)	2664 F	3045 F	2652 F	1731 F
Pellet Temp. (mean)	1642 F	1833 F	1636 F	1176 F
Pellet Temp. (Surface)	-----	-----	620 F	620 F

3.0 DETAIL DESIGN

3.1 Description of the Boiler Fuel Element Assembly

Three types of fuel element assemblies are utilized in the initial boiler core for the Pathfinder reactor. One type, with fuel enriched to 2.2 w/o U-235, is optimized for use in quad box locations but can also be used in single box locations. The others, with fuel enriched to 2.2 and 3.2 w/o U-235 respectively, are designed for use in single box locations only.

Each fuel element assembly includes 81 fuel rods in a 9 x 9 array as shown in Figure 1.3 of ACNP-5905, and in Figure 3 of this report. Each fuel rod is axially segmented into four rod sections. These rod sections are designated as Types I, II, III, and IV numbering from bottom to top. The four fuel rod sections are fastened together over tube sheets by a conventional screwed joint. These fuel rod sections are made of centerless ground UO_2 pellets clad with Zircaloy-2 tubing. End caps for the fuel rod sections are welded to the tubing. Ten types of rod sections are used in the Pathfinder fuel elements and are shown in Figure 4. Various types of rod sections are necessary because there is an axial variation of the neutron flux in the core and consequently the fission gas released varies accordingly. If a fuel rod section were to accommodate the released gases at all locations, a standardized fuel rod would have to be designed for the worst case. This would require a decrease in fuel loading in the average position, which in turn would cause greater local peaking. To avoid these problems, fuel rod sections were optimized for the specific location they would occupy in the core. (This was done only for the 2.2 per cent enriched quad box elements).

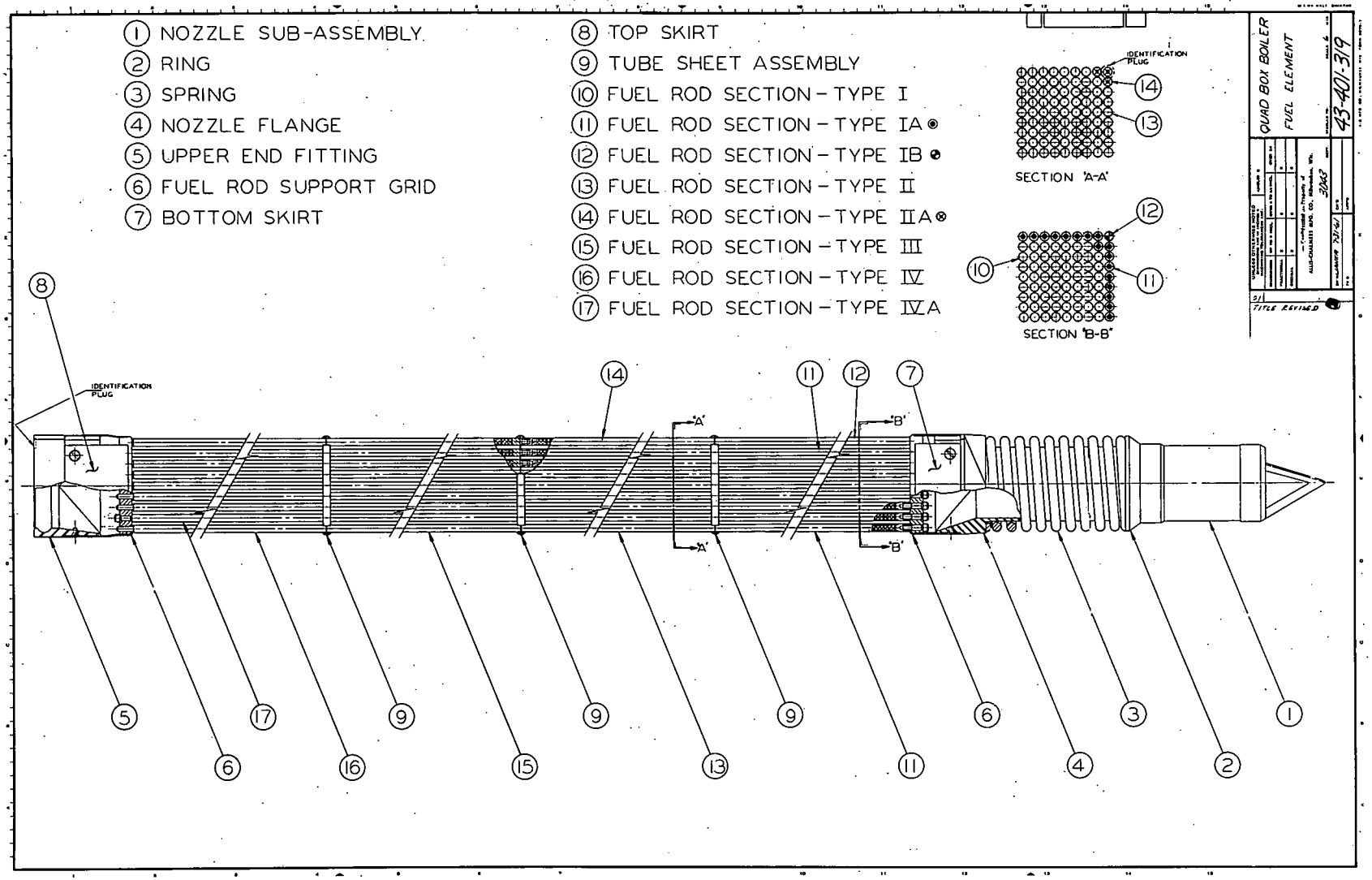

Figure 3...Quad Box Boiler Fuel Element (43-401-319)

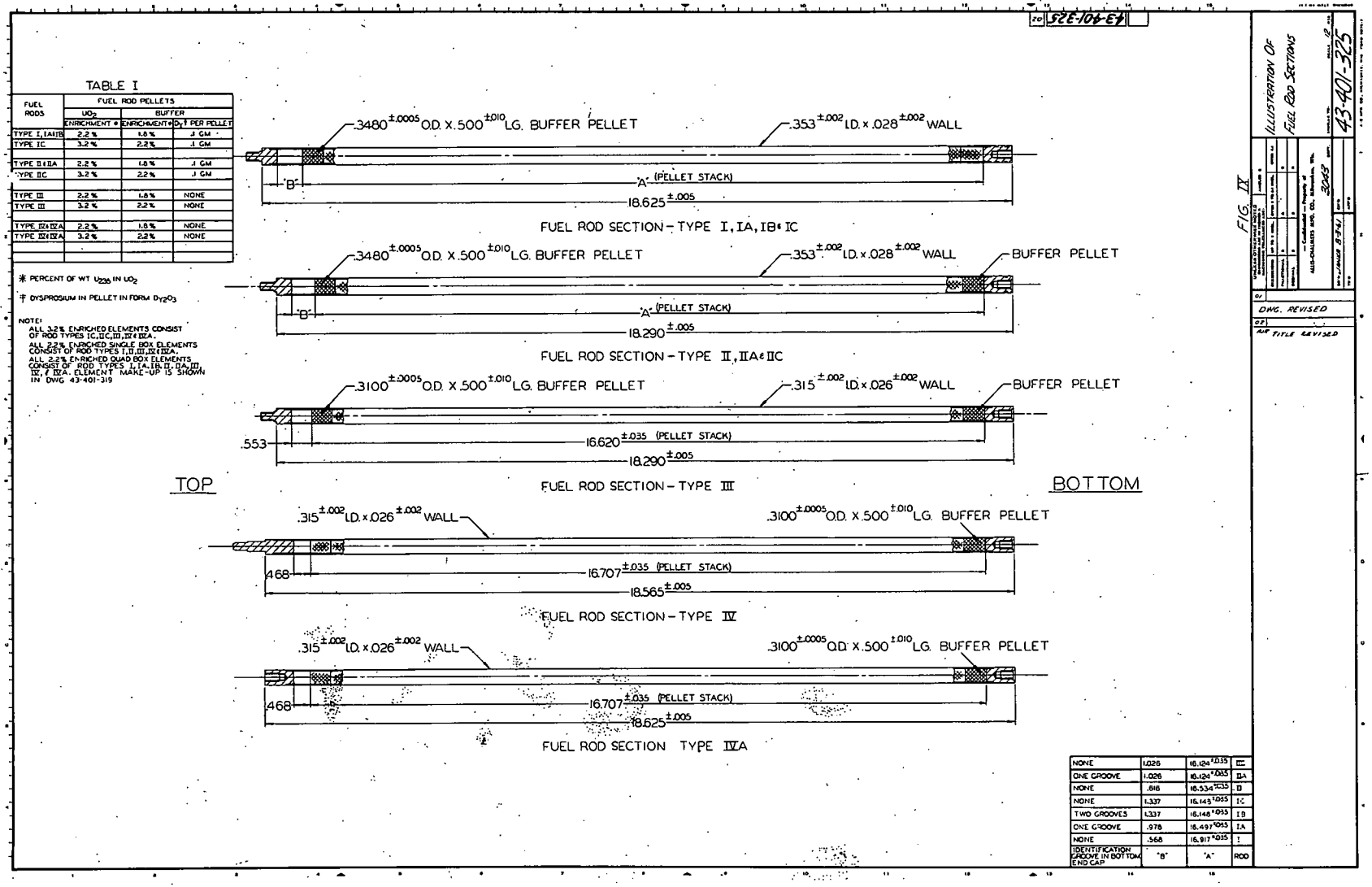

Figure 4...Illustration of Fuel Rod Sections (43-401-325)

The following table shows the various types of fuel rod sections, their designation and the type fuel element in which they are used.

TABLE II

Rod Type	Fuel Element Location	Enrichment
I	Quad and Single Box	2.2%
IA	Quad Box Only	2.2%
IB	Quad Box Only	2.2%
IC	Single Box Only	3.2%
II	Quad and Single Box	2.2%
IIA	Quad Box Only	2.2%
IIC	Single Box Only	3.2%
III	Quad and Single Box	2.2 and 3.2%
IV	Quad and Single Box	2.2 and 3.2%
IVA	Quad and Single Box	2.2 and 3.2%

Fuel rod sections I, IA, etc. and II, IIA, etc. differ from each other only in that each contains a pellet stack of different length. This presents a problem in identification. Fuel Rod Sections IC, IIC, III, IV and IVA of 3.2 per cent enrichment are not identified from their 2.2 per cent counterparts in any manner, so they were processed separately to prevent interchanging with the 2.2 per cent enriched fuel rod sections. Each fuel rod section is also identified by a serial number which is tied in to a particular pellet lot and type of pellet.

A series of grooves turned on the lower end caps, provides a positive means of identifying the Type I and II 2.2 per cent enriched fuel rod sections from

their alternates. Fuel rod Sections I and II do not have the end cap grooves. The lower end caps of Types IA and IIA have a single groove. End cap of Type IB has two grooves. It should be noted that the bottom end caps of Rods I and II differ in that the end cap of Rod I does not contain a counter bore. This prevents switching any of the Rod Type I's with any of the Rod Type II's during assembly. Rod Types III and IV are distinctly different rods with no possibility of being interchanged. Rod Type IVA has female end caps at both ends. However, the top end cap does not contain the counterbore shown in the lower end cap. This prevents the Type IVA rod section from being turned end for end. The diameters of Types I and II are larger than those of Types III and IV, therefore, there is no possibility of interchanging these rods. In addition to the design precautions, extreme care was taken during assembly to insure the correct assembly of the fuel element.

All rod sections, with the exception of Type IV, have buffer pellets adjacent to the fission gas space (Figure 4). The buffer pellets reduce the flux peaks at the rod joints, which among other things, reduces the temperature in the fission gas space. The enrichment and poison loading of the buffer pellets for the various rod sections are listed in the table in Figure 4.

Each rod section contains space to accommodate released gases and differential expansion between the pellet stack and the cladding. Figure 5 shows the fission gas space for each rod section for both the cold and operating conditions.

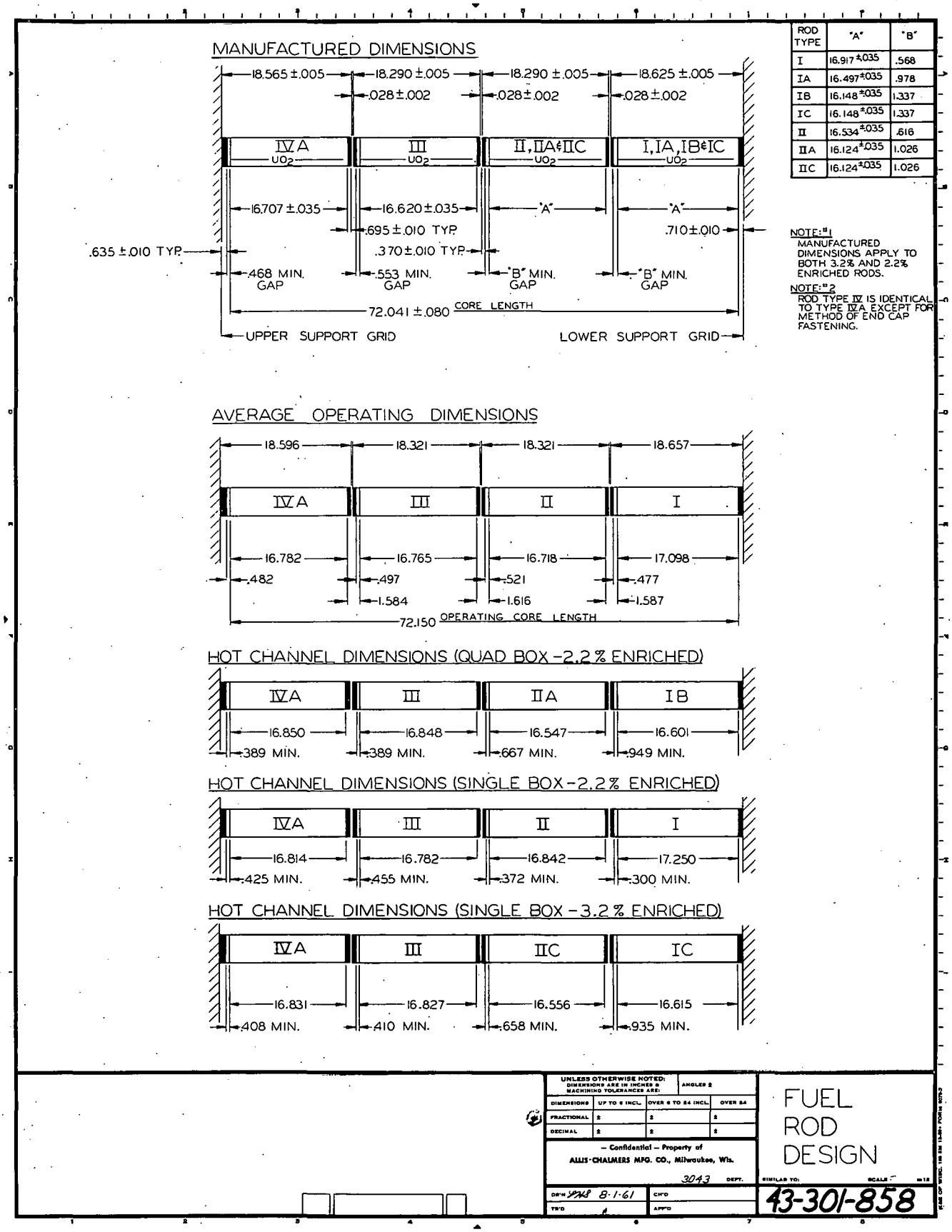

ROD TYPE	"A"	"B"
I	16.917 ±.035	.568
IA	16.497 ±.035	.978
IB	16.148 ±.035	1.337
IC	16.148 ±.035	1.337
II	16.534 ±.035	.616
IIA	16.124 ±.035	1.026
IIC	16.124 ±.035	1.026

NOTE: #1
MANUFACTURED DIMENSIONS APPLY TO BOTH 3.2% AND 2.2% ENRICHED RODS.

NOTE: #2
ROD TYPE IV IS IDENTICAL TO TYPE IV A EXCEPT FOR METHOD OF END CAP FASTENING.

UNLESS OTHERWISE NOTED: DIMENSIONS ARE IN INCHES & MACHINING TOLERANCES ARE: ANGLES ±

DIMENSIONS	UP TO 6 INCL.	OVER 6 TO 24 INCL.	OVER 24
FRACTIONAL	±	±	±
DECIMAL	±	±	±

— Confidential — Property of ALLIS-CHALMERS MFG. CO., Milwaukee, Wis.

3043 DEPT.

DR'N PMS 8-1-61 CH'D

TR'D APP'D

FUEL ROD DESIGN

SIMILAR TO: SCALE

43-301-858

Figure 5...Fuel Rod Design (43-301-858)

The rod bundle has two regions containing rod sections of different diameters. Those in the upper half of the core have reduced diameters to compensate for loss in moderator due to increased steam content.

All fuel element assemblies have a nozzle assembly on the coolant inlet and a handling fitting on the coolant outlet. The fuel handling fitting or upper end fitting is designed to accommodate a quick release pin type handling tool.

The nozzle assembly incorporates a spring which holds the fuel element against the boiler core holddown assembly which, in turn, is supported on the shroud which surrounds the core. The spring offsets the differential thermal expansion between the Zircaloy-2 rod cladding and the stainless steel shroud.

The round-to-square transition of the flange on the nozzle assembly assists in providing a smooth transition from the circular flow channel in the nozzle to the square flow channel in the element. The upper end fitting has a similar transition. The fuel rod support grid for the lower rod bundle is fastened to the nozzle assembly with sheet metal skirts and screws. The upper ends of the fuel rods are spaced by means of a stainless steel grid which is fastened with screws to the upper end fitting.

Mechanical fastening of the fuel rods to the fuel rod support grids is accomplished with bolts. Figure 3 shows the means of attaching the fuel rods to the fuel rod support grids at either end of the element. At the lower end,

all 81 rods are bolted to the support grid, which provides axial and lateral support. At the upper end only 16 of the rods are bolted. The upper fuel rod support grid permits axial movement of the fuel rods. In this manner, the axial restraint is minimized on rods with different thermal expansions (due to local cell and general heat flux variations). The rod bundle is laterally supported every 18.3 inches by 0.028 inch thick tube sheets. The fuel rod sections making up the fuel rod are fastened together over the tube sheets by a conventional screwed joint.

3.2 Fuel Rod

3.2.1 Preliminary Design Consideration

The fission gas generation depends on the number of fissions and the per cent of fission products that are stable gas atoms. The fission gas generation and release are also dependent on the fuel volume. Since the diameter of the fuel rods has been determined, the variation in gas volume is dependent on fuel length. Then, too, the fission product space is dependent on the fuel length. Thus, the determination of the fuel length, the fission space length and the volume of gases released is a reiterative process. The fuel rods are segmented; hence each fuel rod section must have provisions to contain its fission gas release and the thermal expansion of the fuel column without exceeding the allowable internal pressure of the fuel rod section.

The active core length was given as approximately 72 in. This length is measured from the bottom of the fuel stack in Rod Section 1 to the

top of the fuel stack in Rod Section IV. Arbitrary lengths for the end caps for Rod Sections I and IV and fission gas space for Rod Section IV were added to the total core length. This length was then divided by four to obtain an approximate length for each of the four rod sections.

Original design concepts had held the fuel rod sections to equal lengths. End cap design featured snap rings at top and bottom of the fuel rods. All rods were held at the bottom grid by snap rings while only 16 rods were to be held at the top grid by snap rings. However, because of stress corrosion problems and inherent assembly difficulties, the end caps were redesigned. All bottom and 16 top end caps are bolted at the bottom and top end grids, respectively. This, in effect, changed the tubing lengths used in fabricating the fuel rod sections. In order to facilitate process control and standardize on some dimension of the fuel rod, the tubing lengths were made all the same.

Because of mechanical considerations, the lengths of the end caps of the various rod sections are not the same. Hence, the fuel rod sections vary in length. Since the general overall length of the fuel rod sections had been determined, the pellet stack length and fission gas length could be determined. As was mentioned previously, this was a reiterative process. The pellet stack length was arbitrarily chosen. The fission gas generation and release was computed based on this length. The fission gas space had to contain all gaseous products plus provide room for the differential thermal expansion between clad and pellet stack length

without exceeding the allowable internal pressure. If the initial pellet stack length chosen did not satisfy these requirements, then the stack length was adjusted and the process repeated. This was done until all design parameters were met.

3.2.2 Basic Design Criteria

The following criteria were used in making an analysis of the fuel rod:

1. The analysis was based on the hottest rod in the fuel rod bundle.
2. The worst operating criteria, during core life, was selected for each rod section.
3. The UO_2 pellet expansion is based upon the change in volume of the stack.
4. The clad temperature was assumed to be constant for all power distributions and radial hot spot factors. (The actual temperature change was negligible).
5. The pellet surface and inner clad surface were assumed to be at the same temperature. (620 F in all cases).
6. The maximum inside diameter and minimum wall thickness was used.
7. All the fission gas, external to the UO_2 pellets, was assumed to migrate to the fission gas space. No credit was taken for any gap between pellet and clad.
8. The per cent fission gas release was time averaged over the core life. The gaseous release evaluation routine worked out for the IBM-704 computer was utilized. The axial profile of the neutron flux was fed into the core.

9. The total fission gas release was assumed to be present for the worst operating case. This is theoretically possible because of fuel element reshuffling and control rod programming.

10. A smeared thermal conductivity of 1.0 Btu/hr-ft-^{o}F was assumed for the UO_2 pellets.

11. An average gas temperature was computed for the fission gas space. The temperature was based on conduction and radiation phenomena. An IBM-704 computer code was used to obtain temperature profiles through the gas space. Numerical integration techniques were then utilized to calculate the average gas temperature.

12. Mechanical factors for overpower and rod manipulation were included in the hot channel factors.

13. The moisture content of the UO_2 pellet and helium backfill in the rod were considered in determining the total volume of gases.

14. The allowable internal pressure was calculated by an IBM-1620 computer which considered end effects of capped tubing.

15. The gaseous products were assumed to act as a perfect gas.

3.2.3. Fuel Rod Diameter

The criteria for the mechanical design of the fuel rod sections were the overall cold length of the fuel (72 in.) and the diameter of the fuel pellets at the average operating temperature.

These dimensions are0.3115 in. and 0.350 in. for the lower and upper half of the core, respectively. These criteria were established by heat transfer and nuclear physics considerations.

Using the values in Table I, the radial expansion of the pellet was determined. The analysis of the radial thermal expansion of uranium dioxide pellets was performed by assuming parabolic heat generation and no axial or radial restraints. The analysis that follows was performed on the lower half of the core for the maximum hot spot factor.

The general equation of a parabola is given as $y = Ar^2 + B$. One can assume that this equation describes the profile of the thermal neutron flux and volume heat generation through the pellet (Figure 6). B equals the constant flux and Ar^2 equals the value of flux at any radial position. If the maximum radius of the pellet is b, then the maximum neutron flux at this point is Ab^2 and the total neutron flux is $Ab^2 + B$. By definition, the centroid of a parabola, taken from the vertex, is 2/3 h where h is the height of parabola. The average value of the total neutron flux, $\bar{y}$, is then given by:

$$(1) \quad \bar{y} = 2/3\ Ab^2 + B$$

and is located at the radial position $2/3\ Ab^2$.

Similarly for parabolic heat generation, the average heat generation at a hot spot can be given by an equation identical in form to that given above. The average heat generation can also be calculated on the basis of the total power in the boiler and volume of fuel in the core. The average heat generation at the hot spot is then given by:

$$(2) \quad \bar{S} = 3.62 \times 10^5 \ \frac{P \times HSF \times PF}{NFR \times D^2 \times L}$$

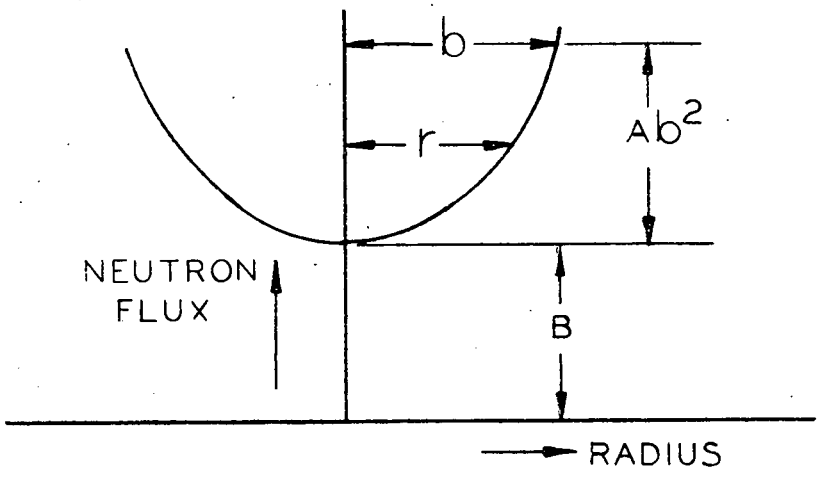

Figure 6...Parabolic Neutron Flux Profile Through the Pellet (43-025-884)

Where:

$\bar{S}$ = Average volumetric heat generation at the hot spot

P = Core power = 157.4 MW

HSF = Total hot spot factor = 3.5

PF = Power fraction = 71% for bottom core half

NFR = Number of fuel rods = 15,552

D = Diameter of pellet cold = 0.348"*

L = Length of fuel rod = 1.5 ft.

Calculating $\bar{S}$ on the basis of the above data gives a value of 5.012×10^4 Btu/hr-in^3 average heat generation at the hot spot. Now the average heat generation and the average neutron flux can be equated to each other by dividing by a constant. Hence,

$$(3) \quad \bar{S} = \frac{\bar{y}}{C}$$

where C is the constant.

This is true since both heat generation and neutron flux were assumed to be represented by parabolic curves. Then from the Equations 1 and 3, the following form can be written

$$(4) \quad \bar{S} = \frac{2}{3} \frac{Ab^2}{C} + \frac{B}{C}$$

$$\text{now let } \frac{A}{C} = N$$

$$\frac{B}{C} = M$$

*The cold pellet diameter was computed by the same method being presented. However, the diameter of the pellet at average operating temperatures (given by physics considerations) and a hot spot factor of one were used in the analysis.

Then the following equation describing the volumetric heat generation through the pellet can be written.

$$(5)\quad \bar{S} = \frac{2}{3} Nb^2 + M$$

Figure 7 was plotted utilizing physics data generated for this particular case. The values of Ab^2 and B can be read directly from this curve.

$$B = 0.8565$$

$$Ab^2 = 0.9125 - 0.8565 = 0.0560$$

then from Equation 1, $\bar{y} = 0.8938$.

The value of $\bar{S}$ was found to be 5.012×10^4, hence C can be determined by using Equation 3.

The value of C was computed to be 1.783×10^{-5}. The values of M and N, constants due to the parabolic heat generation, can now be computed and were found to be 48,037 and 96,171, respectively.

These constants are used in the following equation to determine the pellet diameter at the hot spot. It should be noted that the curve in Figure 7 was extrapolated to give values of neutron flux for diameters larger than 0.168".

Equation 6 was used in the pellet diameter analysis.[1]

$$(6)\quad \Delta r = \frac{\alpha}{24\,K\,(1-\nu)} \left[-\nu Nb^5 + Mb^3\,(3-4\nu) + 24\,bK\,(1-\nu)T_b \right]$$

Where:

Δr = change in radius

α = coefficient of thermal expansion

1. Superscripts refer to references at end of report

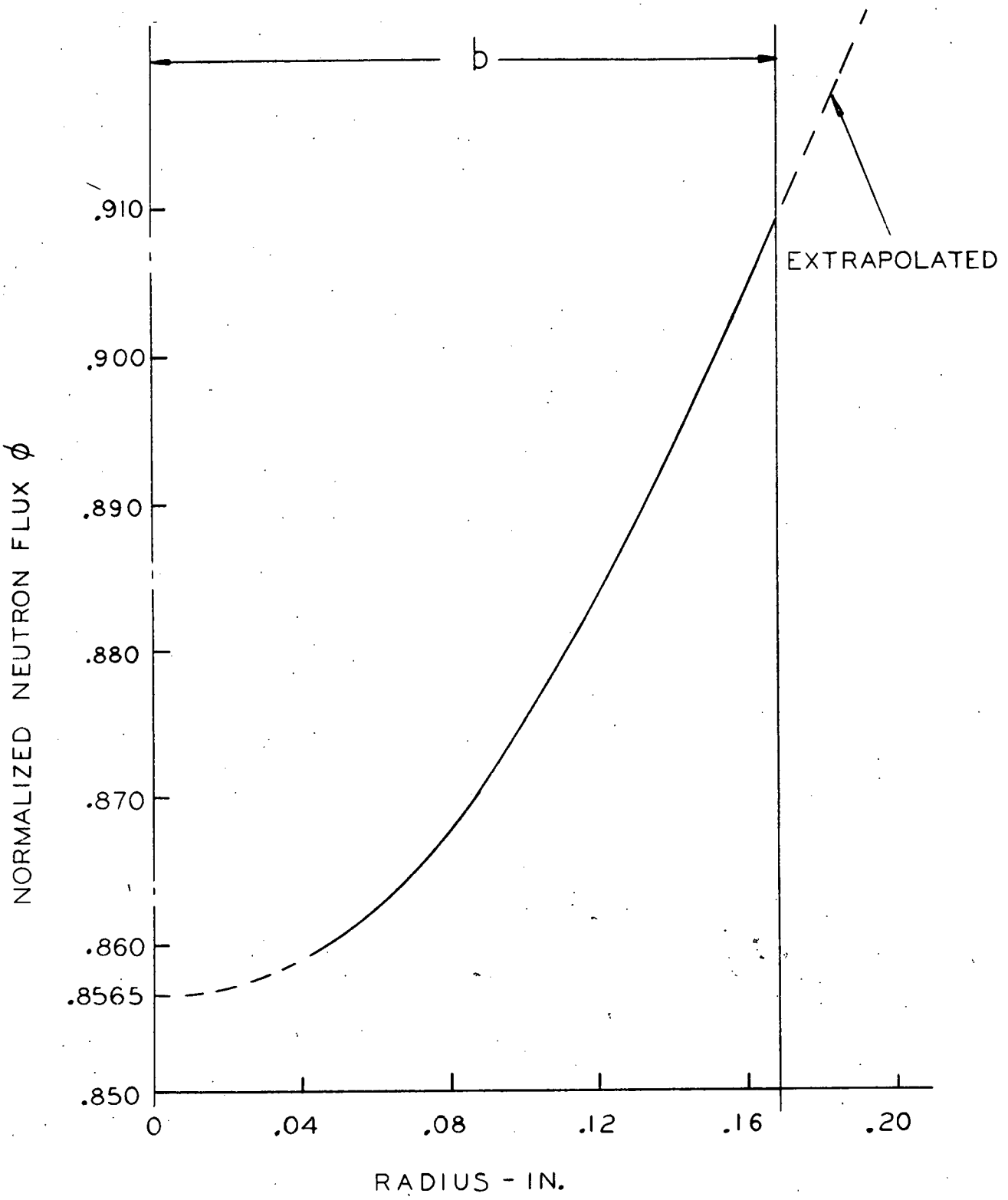

Figure 7...Flux Profile Through Pellet for Pathfinder Conditions (43-025-878)

K = thermal conductivity

ν = Poisson's ratio

b = outside radius of pellet

T_b = surface temperature of pellet

M, N = constants due to parabolic heat generation

The use of this analysis yielded manufacturing or cold pellet diameters of 0.348 in. and 0.310 in. for the lower and upper core halves, respectively. Pellet diameters at the hot spot were computed to be 0.352 and 0.313 for lower and upper core halves, respectively. In order to determine the inside diameter of the Zircaloy-2 clad, a minimum diametral clearance of 0.0025 in. for the insertion of the pellets and manufacturing tolerances of $\pm$ 0.0005 in. on the pellets and $\pm$ 0.002 for the tube were added to the cold diameter of the pellets. This yielded a clad ID of 0.353 and 0.315 $\pm$ 0.002 in. for the lower and upper pins, respectively.

3.2.4 Clad Thickness

The cladding of the fuel rods was designed to be free standing, i.e., to withstand external pressure without requiring support by the UO_2 pellets.

The clad wall thickness was determined after consideration of stresses due to external pressure during corrosion testing. The fuel tubes are autoclaved at 1600 psi and at 750 F. The stress due to external pressure was plotted as a function of wall thickness (Figure 8) using

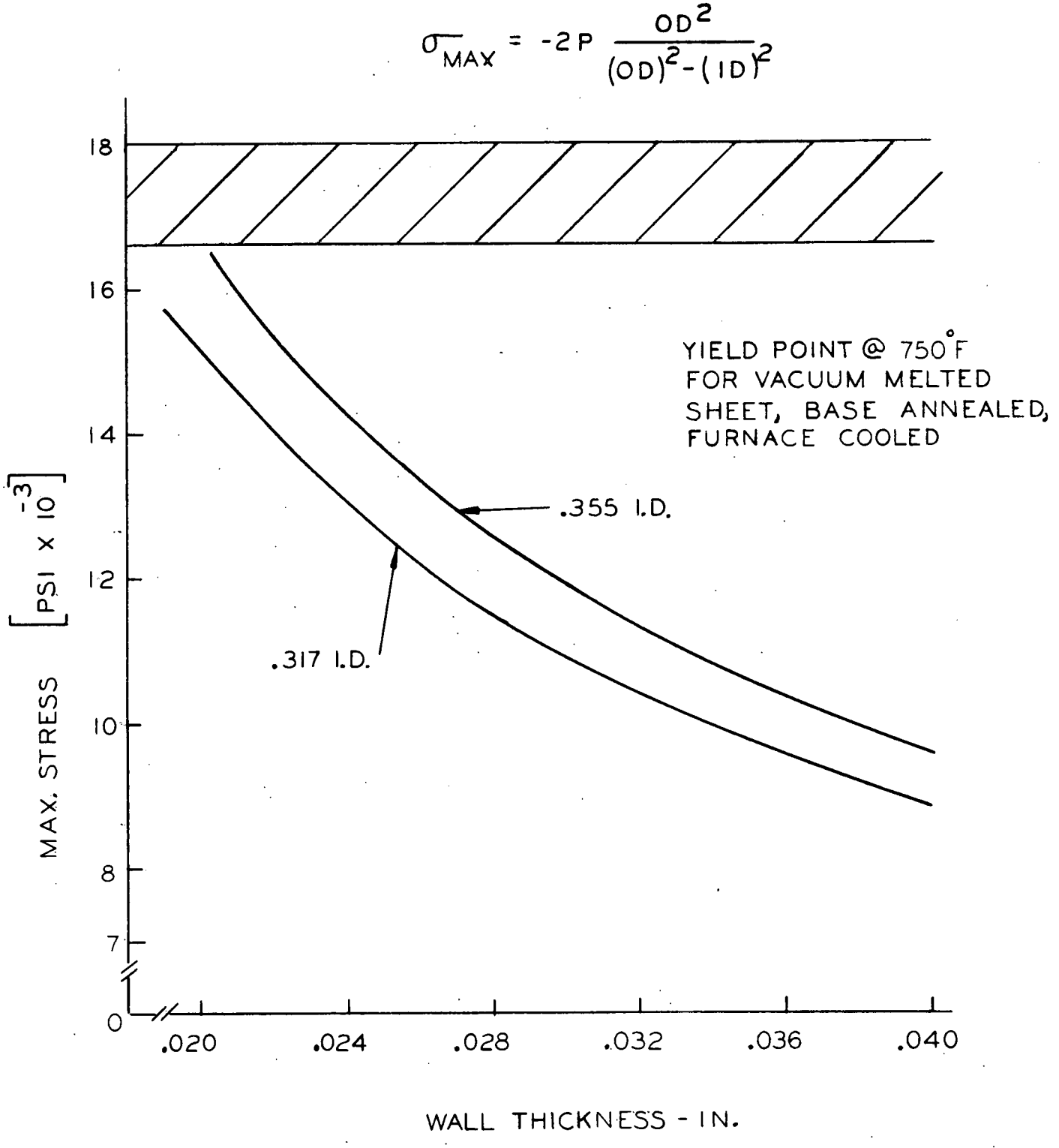

Figure 8...Graph of Clad Wall Thickness vs Clad Stress (43-025-879)

the equation:[2]

$$(7)\quad \sigma_\theta = \frac{2P\, d_2^{\,2}}{d_2^{\,2} - d_1^{\,2}}$$

Where:

σ_θ = tangential stress

P = external pressure = 1600 Psi

d_2 = outside diameter = $d_1 + 2t$

d_1 = maximum inside diameter (0.317 in., 0.355 in.)

t = wall thickness ($0.020 \leq t \leq 0.040$)

Wall thickness of 0.028 ± 0.002 in. for the 0.353 ID tube and 0.026 ± 0.002 in. for the 0.315 ID tube were picked from Figure 7. This choice was based on .8 of the yield strength. It should be noted that the above formula is a specialized case of Lame's formula (thick wall formula) for external pressure only. The range of wall thicknesses selected in the analysis dictates that thick walled criterion be employed. (Wall thickness is greater than ten per cent of the inside radius). Hence, the mode of failure is not elastic collapse, but the reaching of yield stress within the clad wall.

Subsequent to this analysis, a more sophisticated computer code was derived to calculate the wall thickness. The results obtained showed that the tube walls could have been slightly thinner. However, the difference in thickness was too small to justify a change.

3.2.5 Fuel Rod Ovality

With the wall thicknesses determined from external pressure considerations, it was necessary to determine what would be the effect of tube ovality and how much ovality could be tolerated. The maximum allowable ovality was determined using the equation:[3]

$$(8)\quad \bar{W} = \frac{2\bar{S}\,(t/D)}{1 + \frac{4A_o}{t}\,\frac{E\left[N^2-1+\mu\,\frac{\pi^2R^2}{L^2}\right](t/D)^3}{(1-\mu^2)\,(W_c - \bar{W})}}$$

Where:

A_o = ovality = $\frac{D_l - d}{4}$

D = mean diameter = $\frac{D_l + d}{2}$

D_l = major diameter

d = minor diameter

E = modulus of elasticity = 10.3×10^6 Psi

D = average diameter = ID + t

L = length of fuel rod = 17.25 in.

N = Number of lobes = 2

R = mean radius = D/2

$\bar{S}$ = allowable total stress = 16,000 psi

t = wall thickness

$\bar{W}$ = allowable pressure on out-of-round tube

W_c = critical pressure for elastic failure = $\frac{2E}{1-\mu^2}(t/D)^3$

μ = Poisson's ratio = 0.45

This equation is plotted in Figure 9 showing A_o vs $\bar{W}$. In order to further evaluate the effects of ovality, a series of curves were plotted showing "t" vs "$\bar{W}$" with constant ovality (Figures 10 and 11). A curve of critical pressure, W_c, vs thickness, t, was also plotted (Figure 12). Inspection of these curves showed the maximum allowable ovality to be 0.001 in.

3.2.6 Allowable Internal Pressure

The diameters and clad thickness for each rod section were discussed in Section 3.2.4. The diameter and wall thicknesses were determined by the mechanical configuration of the core and the fabrication procedures used in the manufacture of the fuel elements, i.e., final autoclave pressure.

Since the wall thicknesses and diameters of the various fuel rods have been established, the allowable internal pressure of these rods can be computed. The maximum inside diameter and minimum wall thicknesses were used for each case. End restraint of the tube was considered; hence the maximum tubing stress occurred at the clad-end cap interface. This stress includes bending stresses due to the circumferential strain and pressure stresses due to the differential pressure acting across the wall.

The fuel rods are closed on each end by an end cap which is thick enough to be considered rigid in comparison to the rod walls. It was decided that a plot of the stresses versus tube length should be obtained in

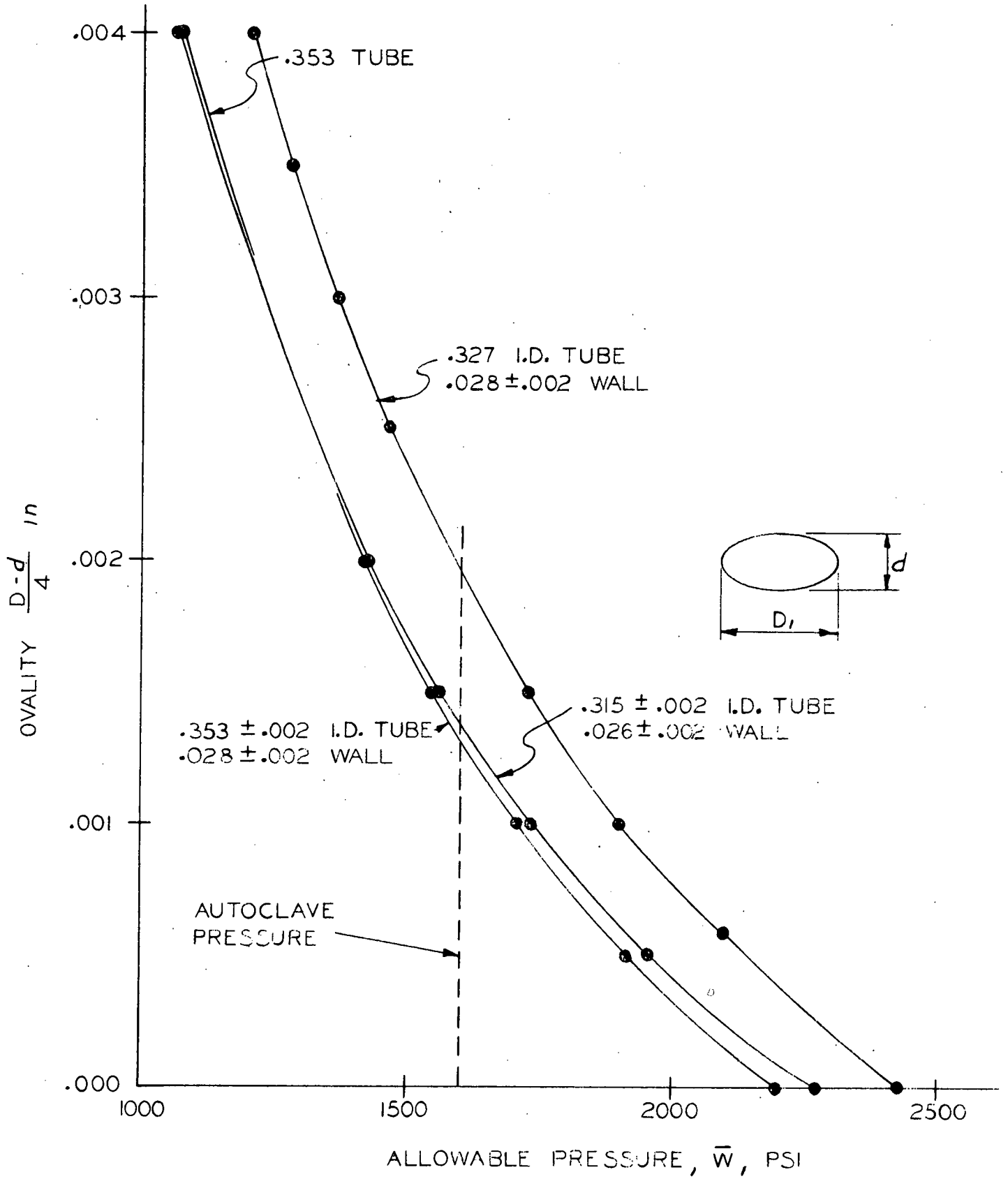

Figure 9...Graph of Allowable Pressure vs Ovality for the Fuel Rod Cladding (43-024-691)

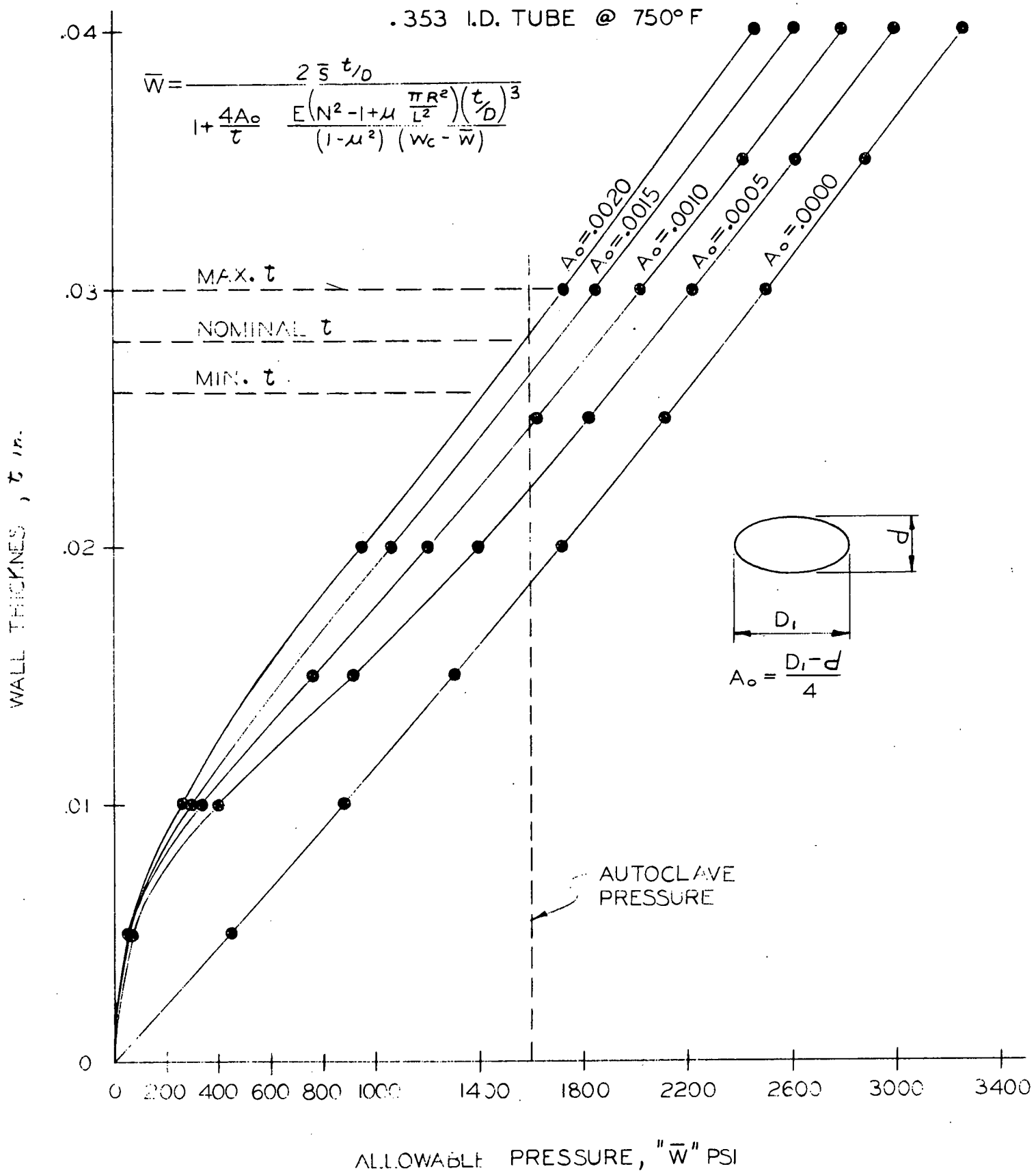

Figure 10...Graph of Allowable Pressure vs Wall Thickness for Fuel Rod Cladding (43-024-692)

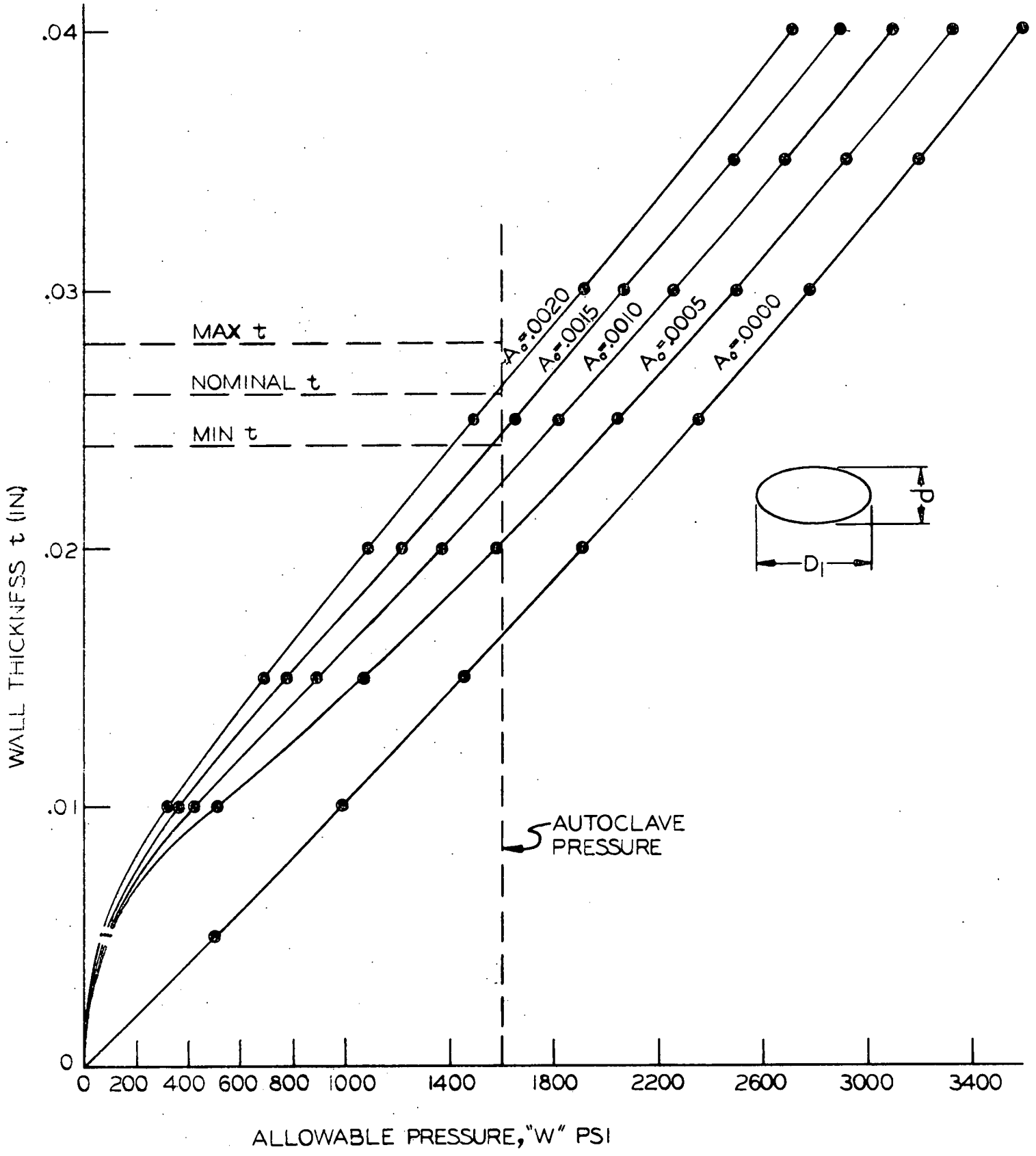

Figure 11...Graph of Allowable Pressure vs Wall Thickness for Fuel Rod Cladding (43-024-689)

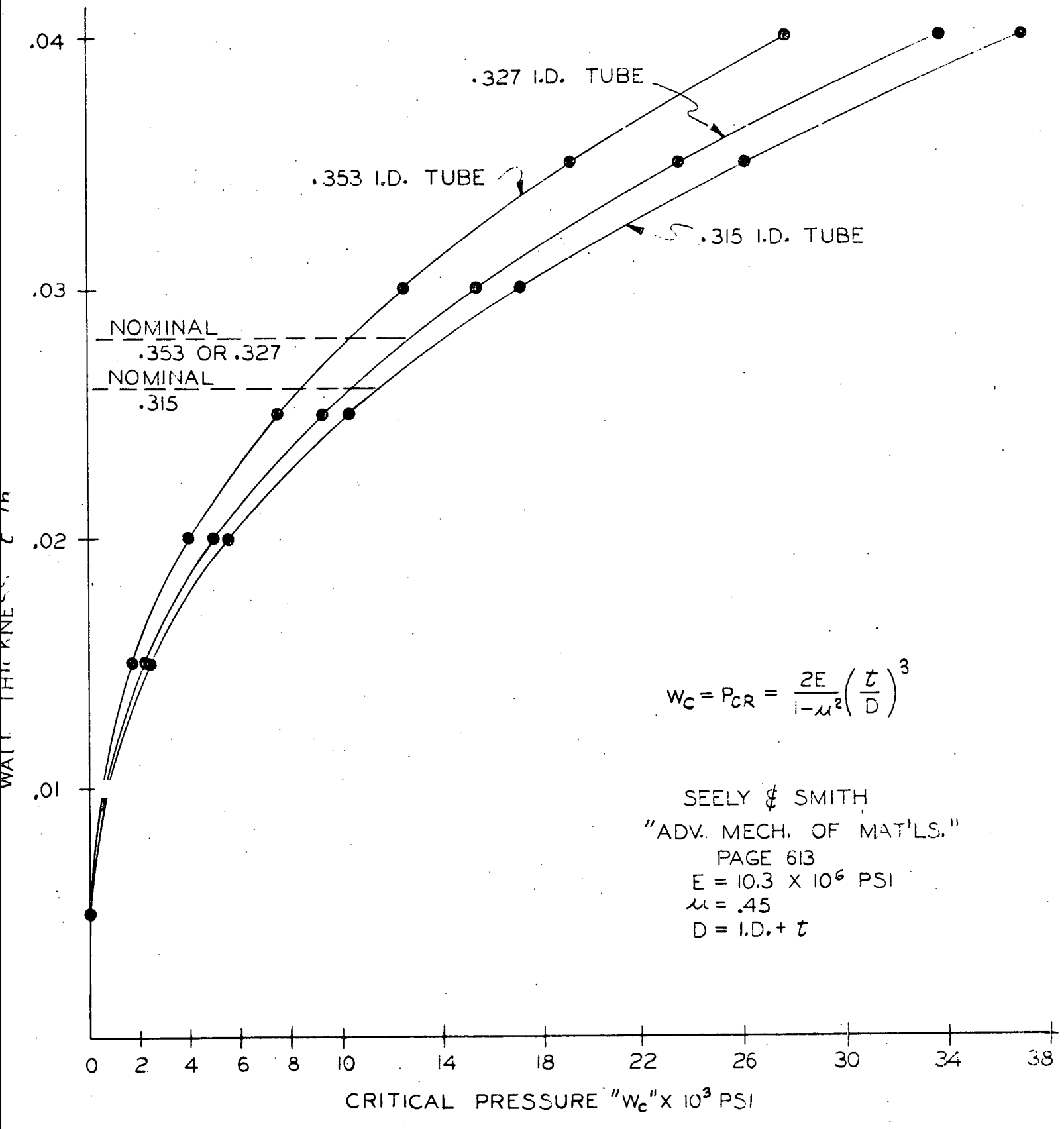

Figure 12...Graph of Critical Pressure vs Wall Thickness for Fuel Rod Cladding (43-024-693)

order to determine the location of the maximum stress. The plot was derived in the form of σ/P where σ is the component stress and P is the differential pressure across the tube wall. The allowable internal pressure is then determined by setting the above term equal to the allowable stress of the tube. The following equation was used in computing the internal pressure.

$$(9) \quad \sigma_A = \sigma/P \ (\Delta P) + P_I$$

where σ_A = allowable stress in tube walls

σ/P = unit pressure

ΔP = differential pressure across tube wall, $P_I - P_E$

P_I = internal pressure

P_E = external pressure

The allowable stress of Zircaloy-2 was taken to be 0.9 the yield stress at 570 F. It was also determined that the maximum total stress due to the end effects (i.e., discontinuity forces, thermal stress and the pressure stress) is below the yield stress for all conditions.

The plot of the unit pressure stress (σ/P) versus tube length was obtained by utilizing a semi-infinite cylinder computer program. The code in essence assumes that the tube walls are held rigidly by the end cap and the axial and circumferential or hoop stress components are calculated on this premise. The results are shown on Figures 13 and 14. With the maximum stress (axial) occurring at the clad-tube interface,

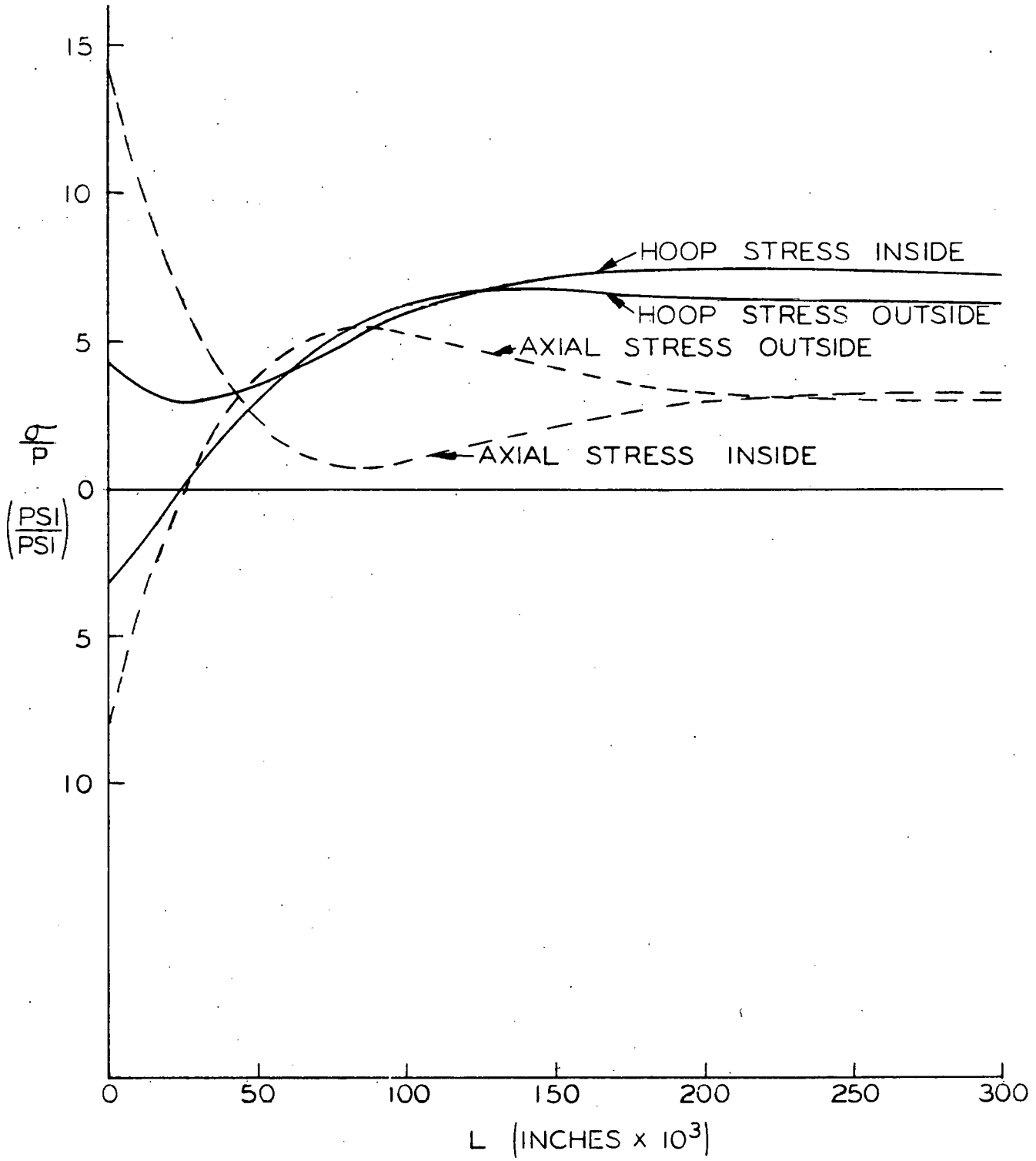

Figure 13...Graph of Unit Pressure Stress vs Distance from End Cap Rods I and II (43-025-442)

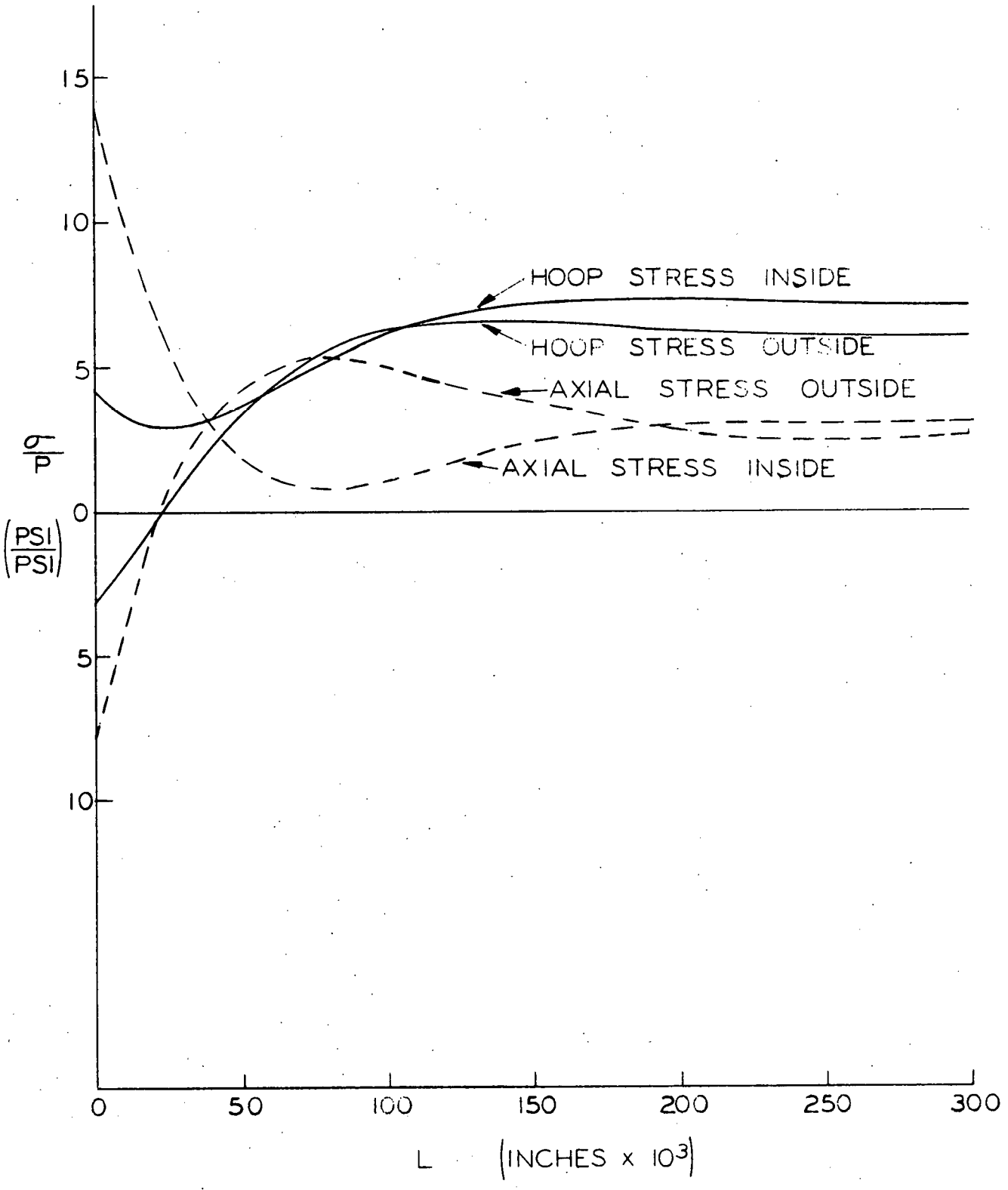

Figure 14...Graph of Unit Pressure Stress vs Distance from End Cap Rods III and IV (43-025-443)

the maximum allowable pressures are 1600 psi for Rod Sections I and II and 1650 psi for Rod Sections III and IV.

The computer code used to calculate the values of unit pressure stress, σ/P, was a two-part code. The first portion of the code is used to solve for the discontinuity forces. These are the moment and shear forces at the fixed end. The moment and shear forces are then entered into a second program, along with other data, and the unit pressure stress, σ/P, is computed for .050 in. increments along the length of the tube out to 1/4 inch. The axial and hoop stresses, (given in terms of σ/P) both inside and outside are calculated. The following pages show the format of the aforementioned codes and also show a print-out for each one.

3.2.7 Cladding Stress

A summary of the stress in the cladding (assuming infinite tube length) was made which includes both pressure and thermal stresses. The equations used were:

Inside stress due to temperature drop across clad.[4]

$$(10)\quad \sigma_a = \frac{E\,\alpha}{2\,(1-\mu)} \times f_2\,(t_b - t_a) \qquad f_2 = 1.051$$

Outside stress due to temperature drop across clad.[5]

$$(11)\quad \sigma_b = \frac{E\,\alpha}{2\,(1-\mu)} \times f_3\,(t_b - t_a) \qquad f_3 = -.949$$

```
   SEMI-INFINITE CYLINDER  INFLUENCE COEFFICIENTS
   J.GEORGE  D.BRUESEWITZ    11/26/62
 1 FORMAT(F6.3,F5.3,E6.0,F4.0)
 2 FORMAT(3H D=,E11.4//3H B=,E11.4//3HPD=,E11.4//)
 3 FORMAT(11X3HBM1,13X2HQ1)
 4 FORMAT(5HDEL1=,2XE11.4,4XE11.4/5HANG1=,2XE11.4,4XE11.4//)
 5 FORMAT(47HSEMI-INFINITE CYLINDER - INFLUENCE COEFFICIENTS///)
 6 FORMAT(38HDESCRIPTION OF CYLINDER BEING ANALYZED/)
 7 FORMAT(13HINSIDE RADIUS,5XF8.3,7X6HINCHES)
 8 FORMAT(14HWALL THICKNESS,5XF7.3,7X6HINCHES)
 9 FORMAT(14HYOUNGS MODULUS,5XE12.4,2X3HPSI)
10 FORMAT(15HDESIGN PRESSURE,5XF6.0,7X3HPSI//)
11 FORMAT(//15HEND OF ANALYSIS/)
   READ1,RI,TH1,E,P
   PRINT 5
   PRINT 6
   PRINT 7,RI
   PRINT 8,TH1
   PRINT 9,E
   PRINT10,P
   RM=RI+TH1/2.
   D=E*TH1**3/10.92
   B=1.285/(RM*TH1)**.5
   PD=-P*RM**2*.85/(E*TH1)
   PRINT2,D,B,PD
   U=.5/(B**2*D)
   C1=-U
   C2=-U/B
   C3=2.*U*B
   C4=U
   PRINT 3
   PRINT4,C1,C2,C3,C4
   PRINT11
   STOP
   END
```

SEMI-INFINITE CYLINDER - INFLUENCE COEFFICIENTS

DESCRIPTION OF CYLINDER BEING ANALYZED

INSIDE RADIUS	.180	INCHES
WALL THICKNESS	.018	INCHES
YOUNGS MODULUS	26.0000E+06	PSI
DESIGN PRESSURE	1.	PSI

D= 1.3885E+01

B= 2.2031E+01

PD=-6.4877E-08 ← PRESSURE INFLUENCE COEFF.

	BM1	Q1
DEL1=	-7.4187E-05	-3.3673E-06
ANG1=	3.2688E-03	7.4187E-05

END OF ANALYSIS

STOP

```
      DIMENSION X(16)
    1 FORMAT(F6.3,F5.3,E6.0,F4.0,E10.4,E10.4)
    2 FORMAT(6HSHMO= ,E11.4/6HSHMI= ,E11.4/6HSAM = ,E11.4//)
    3 FORMAT(2HX=,F6.2,4XE11.4,4XE11.4,4XE11.4,4XE11.4/)
    4 FORMAT(16X36HSTRESSES IN A SEMI-INFINITE CYLINDER///)
    5 FORMAT(38HDESCRIPTION OF CYLINDER BEING ANALYZED/)
    6 FORMAT(13HINSIDE RADIUS,5XF8.3,7X6HINCHES)
    7 FORMAT(14HWALL THICKNESS,5XF7.3,7X6HINCHES)
    8 FORMAT(14HYOUNGS MODULUS,5XE12.4,2X3HPSI)
    9 FORMAT(15HDESIGN PRESSURE,5XF6.0,7X3HPSI)
   10 FORMAT(18HEND BENDING MOMENT,2XE11.4,2X8HIN-LB/IN)
   11 FORMAT(15HEND SHEAR FORCE,5XE11.4,2X5HLB/IN//)
   12 FORMAT(16X3HSHO,12X3HSHI,12X3HSAO,12X3HSAI/)
   13 FORMAT(//15HEND OF ANALYSIS/)
      READ1,RI,TH1,E,P,BM1,Q1
      PRINT 4
      PRINT 5
      PRINT6,RI
      PRINT7,TH1
      PRINT8,E
      PRINT9,P
      PRINT10,BM1
      PRINT11,Q1
      RM=RI+TH1/2.
      D=E*TH1**3/10.92
      B=1.285/(RM*TH1)**.5
      U=.5/(B**2*D)
      YY=(RI+TH1)/RI
      SAM=1./(YY**2-1.)*P
      SHMI=(YY**2+1.)/(YY**2-1.)*P
      SHMO=2.*SAM
      PRINT2,SHMO,SHMI,SAM
      PRINT12
      X(1)=0.
      X(2)=.25
      X(3)=.5
      X(4)=1.
      X(5)=2.
      X(6)=3.
      X(7)=4.
      X(8)=5.
      X(9)=6.
      X(10)=8.
      X(11)=10.
      X(12)=14.
      X(13)=18.
      X(14)=22.
      X(15)=26.
      X(16)=30.
      DO 15 I=1,16
      Y=B*X(I)
      SX=COS(Y)/(2.718**Y)
      TX=SIN(Y)/(2.718**Y)
      QX=SX+TX
      RX=SX-TX
      DELX=-U*BM1*RX-U*SX*Q1/B
      BMX=BM1*QX+Q1*TX/B
      SHO=SHMO-E*DELX/RM-1.8*BMX/(TH1**2)
      SAO=SAM-6.*BMX/TH1**2
      SHI=SHMI-E*DELX/RM+1.8*BMX/(TH1**2)
      SAI=SAM+6.*BMX/TH1**2
   15 PRINT3,X(I),SHO,SHI,SAO,SAI
      PRINT13
      STOP
```

STRESSES IN A SEMI-INFINITE CYLINDER

DESCRIPTION OF CYLINDER BEING ANALYZED

INSIDE RADIUS	.180	INCHES
WALL THICKNESS	.018	INCHES
YOUNGS MODULUS	26.0000E+06	PSI
DESIGN PRESSURE	1.	PSI
END BENDING MOMENT	8.7600E-04	IN-LB/IN
END SHEAR FORCE	-3.8600E-02	LB/IN

SHMO= 9.5238E-00
SHMI= 1.0523E+01
SAM = 4.7619E-00

UNIT PRESSURE STRESSES		HOOP STRESS OUTSIDE	HOOP STRESS INSIDE	AXIAL STRESS OUTSIDE	AXIAL STRESS INSIDE
X=	.00	-4.2837E-00	6.4496E-00	-1.1460E+01	2.0984E+01
X=	.05	6.2408E-00	5.8180E-00	7.1332E-00	2.3905E-00
X=	.10	1.0062E+01	9.5592E-00	7.2670E-00	2.2567E-00
X=	.15	1.0048E+01	1.0753E+01	5.2530E-00	4.2707E-00
X=	.20	9.6220E-00	1.0699E+01	4.6327E-00	4.8910E-00
X=	.25	9.4953E-00	1.0551E+01	4.6688E-00	4.8549E-00

Stress due to axial temperature drop.[6]

$$(12)\quad \sigma_z = 1/2\ \alpha\ E\ \Delta T_d$$

Stress due to Internal Pressure.[7]

$$(13)\quad \sigma_t = \frac{P_1 a^2 - P_2 b^2 + a^2 b^2/P^2\ (P_1 - P_2)}{b^2 - a^2}$$

$$(14)\quad \sigma_z = \frac{P_1 a^2 - P_2 b^2}{b^2 - a^2}$$

where

a = inside radius

b = outside radius

E = 10.3×10^6 psi

f = factor which is function of I.D./O.D.

P_1 = internal pressure (previous section)

P_2 = external pressure

ΔT_d = axial temperature change in one diameter

t_a = temperature at inside radius

t_b = temperature at outside radius

α = coefficient of thermal expansion

μ = Poisson's Ratio

P = general radius (value depends on whether stress is wanted at the inner or outer tube surface).

σ = stress

σ_a = thermal stress at inside, tangential and axial

σ_b = thermal stress at outside, tangential and axial

σ_z = axial thermal stress due to ΔT_d

σ_x = axial pressure stress

σ_t = tangential pressure stress

The solutions of these equations for all combinations of minimum, nominal and maximum inside diameters, and minimum, nominal and maximum wall thicknesses resulted in maximum hoop stresses of 12,760 psi in the 0.353 in. ID by .026 in. wall tube and 12,786 psi in the .317 in. ID by .024 in. wall tube. Maximum axial stresses were 12,758 psi and 11,994 psi in the .353 in. ID and .317 in. ID tubes respectively. All these stresses are below the yield stress of Zircaloy-2 at operating temperature. The previous equations and subsequent maximum stresses did not include end effects which are present in tubes of finite length. However, these effects were considered in Section 3.2.6 in determining allowable internal pressure, such that the yield stress of the cladding is not exceeded by the maximum internal pressure.

3.2.8 Fission Gas Generation and Release

As mentioned previously, the generation of gas atoms per rod is dependent on the burnup in the fuel rod, the amount of UO_2 in the rod and the number of stable fission products produced per fission. This information was generated by the Physics Section. Since the fuel stack is not known initially, it must be approximated. This approximated length is also used to calculate the length of the hot fission gas space. (It should be noted that fission gas generation and release increase with stack length. However, the increase in stack length is small, such that the increase in gases is negligible, and the approximate cold length was used).

The fission gas release within all Pathfinder fuel rods was determined by the utilization of the IBM-704 GRER (Gaseous Release Evaluation Routine) program.[8] The assumptions intrinsic to the code are as follows:

1. Fission products are assumed to be released by a temperature-dependent diffusion process.
2. Fuel temperatures are determined by assuming only radial heat conduction through the fuel material.
3. Thermal conductivity of UO_2 was assumed to be independent of temperature and was taken as 1.0 Btu/hr-ft-^{o}F.
4. The fuel pellet surface temperature is assumed to be constant along the axial length of the rod.
5. Only stable fission gas products, long half-lives, are considered.
6. Density of UO_2 was assumed constant at 93 per cent of theoretical.
7. A power profile table is used to provide the variation of boiler power with axial length along the boiler fuel rod.

The equivalent - sphere hypothesis, as proposed by Booth,[9] was used as the diffusion model. The equivalent radius of the isothermal spheres is assumed constant for a given uranium dioxide fuel material density and specific surface. Values of the specific surfaces were determined[10] experimentally as a function of the bulk fuel density by Aronson. The diffusion coefficient as determined experimentally has been correlated by the Arrhenius equation. An activation energy of 115,000 cal/mol above

1000 C and 850 cal/mol below 1000 C for xenon and krypton, as suggested by J. D. Eichenburg.

Large temperature gradients, both radially and axially, are present in operating nuclear fuel rods. The sensitivity of the gaseous diffusion rate to temperature and the diffusion model used, required a detailed temperature prediction calculation.

For temperature and fission gas release evaluation purposes, the fuel assembly is divided into four axial elements. The volumetric heat generation within a typical rod within each axial element is determined from the total input channel power and the supplied axial power shape. Time-integrated hot channel factors obtained by physics calculations were employed to thermally describe the hottest boiler fuel rod. As was mentioned previously, the hottest fuel rods in the lower half of the core occur at beginning of life, and end of life conditions are used to describe the hottest fuel rods in the upper half of the core. The axial power shape for all fuel rod sections was calculated from physics considerations and was entered into the code.

The typical rod for each of the axial elements is further subdivided into 20 equal lengths and the volumetric heat generation within each length calculated using the elemental volumetric power and axial power profile. Each incremental length of the fuel pin is then considered

to consist of 10 concentric shells or radial rings of equal wall thickness. As the assumption of constant radial heat generation across the fuel rod has been made, the volumetric heat generation in each shell within a given incremental length is constant.

The temperature for each incremental shell is then calculated, assuming conduction to be the only mode of heat transfer. The UO_2 thermal conductivity was assumed constant independent of temperature and was conservatively taken to be 1.0 Btu/hr/ft/^{o}F. The fuel pellet surface temperature, assumed constant along the axial length of the rod, was taken to be 600 F.

With the fuel temperature established for each cylindrical shell in the fuel rod, the fission gas fractional release is calculated. The diffusion constants for each shell are determined using the previously calculated shell temperature. An irradiation time of 515 days was assumed for all axial elements.

The results of the Pathfinder boiler core fission gas analysis are summarized in Table III. All data is for most severe operating conditions.

TABLE III

	Rod #1	Rod #2	Rod #3	Rod #4
Average UO_2 Temperature	1771 ^{o}F	1694 ^{o}F	1245 ^{o}F	903 ^{o}F
Maximum Centerline Temperature	3217 ^{o}F	3080 ^{o}F	2256 ^{o}F	1684 ^{o}F
Total Fission Gas Release per Element (%)	26.26%	20.70%	2.14%	2.0%

3.2.9 Fission Gas Temperature

An analysis to establish the temperature distribution in the vicinity of the fuel rod end caps was conducted. Of special interest was the temperature profile through the fission gas space. The temperatures were computed on an IBM-704 computer, using the PDQ neutron diffusion program.[11] The calculation made was based on the power generation in the pellet adjacent to the gas space. Both radiation and conduction were considered in the temperature derivation.

The temperature varies with both increase or decrease in the fission gas length and power distribution in the fuel rod section. Here again the interdependence of the various fuel rod parameters is shown.

The temperatures were printed out in a network which simulated the the physical configuration of the end cap, fission gas space and adjacent pellet. This analysis used the hot length of the fission gas space. The radial temperature distribution across the fission gas space was then plotted for a series of axial locations. Figure 15 shows such a plot.

The curves were then numerically integrated to obtain an average fission gas temperature. The curves were integrated by using the system of cylindrical shells, for which the following equation was derived,

$$(15) \quad T_{AVE} = \frac{\Sigma\, 2\pi \bar{R}\, \bar{T}\, dr}{\Sigma\, 2\pi \bar{R}\, dr}$$

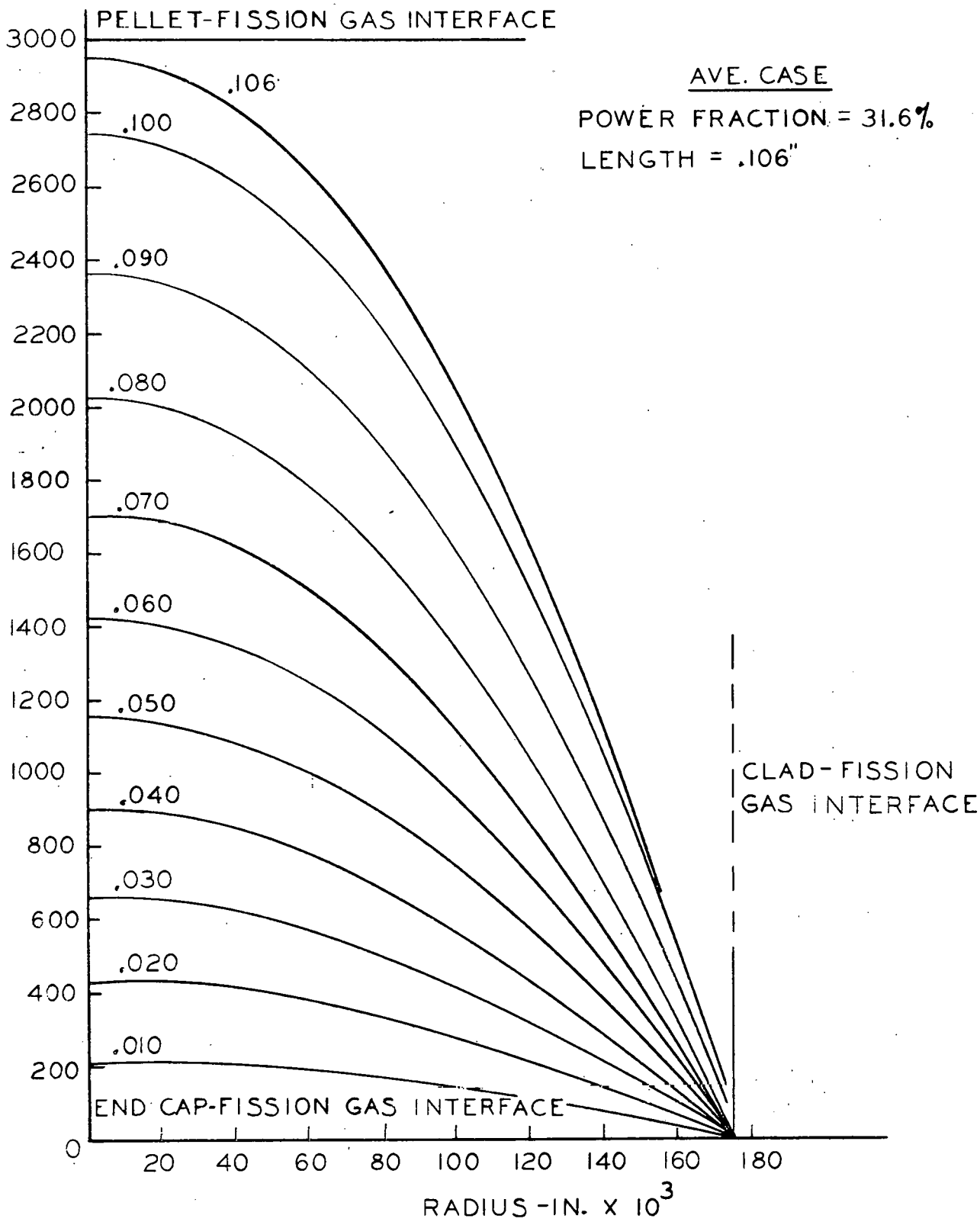

Figure 15...Radial Temperature Distribution in Fission Gas Space (43-025-880)

but dr was chosen as a constant, hence the formula reduces to the following:

$$(16)\quad T_{AVE} = \frac{\Sigma \bar{R}\,\bar{T}}{\Sigma \bar{R}}$$

In the above formula, the only remaining variables are the radius and temperature. As was previously mentioned, the gas temperature does vary with the length of the fission gas space. The temperature was calculated for the smallest fission gas space for each rod section. This temperature was then used for all other operating conditions.

3.2.10 Clad and Pellet Expansion

All design and stress analysis thus far had been concerned with the radial dimensions of the fuel rod. The design which remained was to determine the length of fuel in each rod and the lengths of the rods themselves. There were two major problems in arriving at the length of fuel in the fuel rods. One problem was differential thermal expansion between the fuel and the clad, and the other was that after differential expansion there had to be sufficient space within the cladding to contain the fission gas released during operation. An initial analysis was made to determine the axial thermal expansion of uranium dioxide pellets which used the equation (12);

$$(17)\quad \Delta L = L_o \left[(1 + \mu)\,\alpha T_{\ell} - \mu\alpha T_{AVE} - \alpha T_R\right] = KL_o$$

where:

ΔL = thermal expansion of UO_2

L_o = maximum cold length of UO_2

μ = Poisson's ratio = 0.3

α = thermal coefficient of expansion = 5.8×10^{-6} in/in ^{o}F

T_{ℓ} = centerline temp. ^{o}F

T_{AVE} = average temp. ^{o}F

T_{R} = room temp. ^{o}F

The temperatures are known since they are dependent on the diameters of pellets and cladding, and power level. Through trial and error, an approximate cladding length and an approximate fuel length were known. The end caps had also been designed at this point. Considering the criteria that the overall cold length of the core was to be 72 in., the approximate values were used and a shoulder length on the fuel rods was determined. Since the end cap dimensions were known, this gave a metal-to-metal length inside the rod. The amount of fission gas released was determined as previously described. An equation was then written for the maximum cold length of the UO_2:

$$(18) \quad L_o = L_T - \Delta L - L_{FG}$$

$$= L_T - KL_o - L_{FG}$$

$$L_o = \frac{L_T - L_{FG}}{1 + K}$$

where:

L_T = metal-to-metal hot, minimum

K = $(1 + \mu)\,\alpha T_{\ell} - \mu\alpha T_{AVE} - \alpha T_R$

L_{FG} = length for fission gas

New data on the thermal expansion of UO_2 was acquired after the above analysis was conducted.[13] This data pointed out that the value given for the coefficient of expansion (5.8×10^{-6} in/in°F) was low. In the previous analysis the coefficient of expansion was assumed to be independent of temperature. However, the new data (Figure 16) showed this assumption to be in error and hence the new procedure for calculating the thermal expansion of uranium dioxide was undertaken. It was reasoned that since the equation from Reference 9 assumed that the pellet column is composed of an infinite number of thin discs which offer only radial restraint, that the use of this equation is overly conservative. The result of this radial restraint is that the cooler UO_2 near the surface restrains the hotter material near the center of the pellet from expanding radially. Consequently, the axial expansion at the center is increased by Poisson's ratio as noted in the first term in brackets in Equation 17. Since the actual pellets crack both radially and circumferentially, this radial restraint cannot exist.

A more realistic approach is believed to encompass the change in volume of the stack. It seems reasonable that effective axial expansion may be conservatively calculated by averaging the expansion of the hot half of the UO_2 column ($\Delta L = \alpha_{\bar{T}} T_{\bar{T}} L_o$) and the cool half of the column ($\Delta L = \alpha_{AVE} T_{AVE} L_o$). A parabolic temperature profile exists across the UO_2 pellet thus, half of the pellet will be warmer than T_{AVE} and half will be cooler. Hence the average of these two expansions should be a fair, though conservative estimate of what the pellet column will actually do.

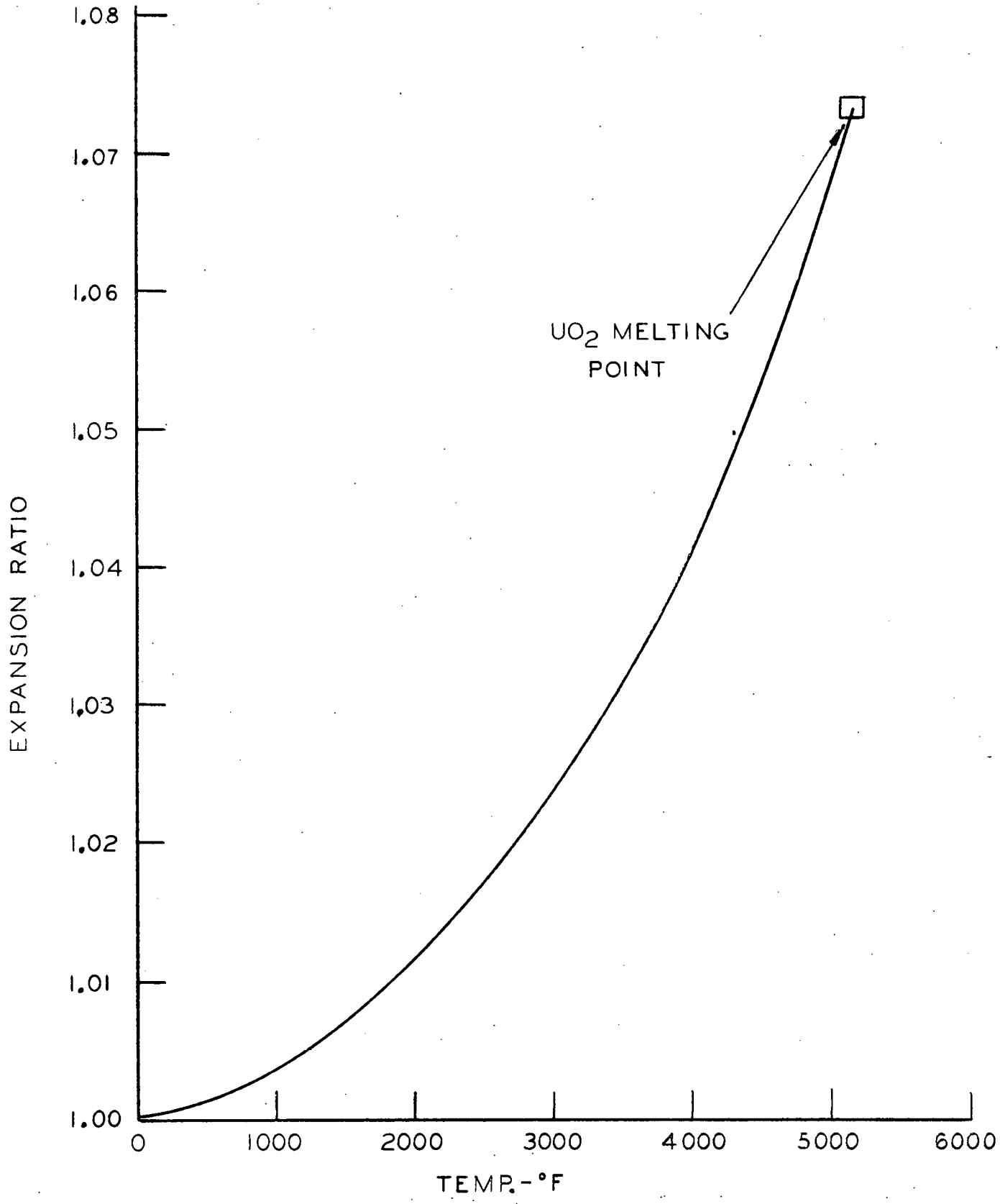

Figure 16...Linear Expansion of UO_2 vs Temperature (43-025-881)

The expansion ratios corresponding to the centerline and average temperatures were selected from Figure 16. The average value of these ratios was then used to determine the hot length of the uranium dioxide column. The cold length of the pellet stack was that used to compute the fission gas generation and release. The maximum expansion for the most severe operating conditions was approximately 7/16 in.

The mean tube temperature, considering the maximum hot spot factors, was calculated to be 569 F and 565 F for the lower and upper core halves respectively. Report HW-60908, "A Report of the Properties of Zircaloy-2", gives a value of 3.41 c 10^{-6} in/in^{o}F for the coefficient of expansion of Zircaloy-2 at 570 F. This is sufficiently close to the temperatures of the clad at both upper and lower core halves so that no correction is necessary. The metal-to-metal dimensions determined earlier are used to compute the increase in length of the clad. (Pertinent data on core and fuel lengths is shown in Figure 5). Subtracting the maximum hot pellet stack length from the minimum metal-to-metal length, hot, gives the minimum fission gas length at temperature. The radial expansion of the cladding was also considered. The area increase was calculated by utilizing the surface coefficient of expansion. Thus, the minimum volume, at temperature can be computed.

3.2.11 Determination of Gas Space

The minimum fission gas space (hot) is the fission gas space cold plus the difference in expansion between the Zircaloy-2 cladding and the UO_2

pellets. The average temperature of the pellets is greater than that of the clad. This factor coupled with Zircaloy-2's relatively low coefficient of expansion results in the pellets expanding more than the cladding. Thus, the fission gas length decreases with temperature.

The fission gas generation and release is a function of the pellet stack length. The gas temperature is dependent on the length of the gas space. Therefore, a reiterative process was utilized in calculating the required gas space. The general rod section length was dictated by the mechanical configuration of the core. Hence, a pellet stack length and fission gas space were chosen, the temperatures and expansions calculated, the fission gas release and temperatures were computed and the volume of the fission gas (hot) was compared with the available volume; if the resulting fission gas pressure exceeded the design pressure, then a new pellet stack length and fission gas space was chosen. The process continued until the fission gas pressure was less than the maximum design pressure. In computing the fission gas space, the diameter of the fuel rod section is fixed. The maximum tube internal diameter and minimum wall thickness were used. This in turn limits the allowable stress in the tube walls and the allowable pressure in the fuel rod tube.

In computing the fission gas pressure, the total volume of gases was used. This includes moisture content of pellets, helium backfill of

fuel rods and the fission gas itself.

Manufacturing procedures dictate backfilling the fuel rods with helium at one atmosphere pressure. Hence by utilizing the maximum internal diameter, credit is given for the maximum volume of helium in the fuel rod section. Therefore, a volume of helium, equal to the fission gas space cold, plus gap between pellet and clad, and converted to standard conditions, must be added to the volume of fission gas.

Manufacturing and handling procedures permit moisture absorption by the UO_2 pellets. Hence, a pellet-drying procedure has been incorporated into the manufacturing sequence just prior to welding the second end cap onto the rod sections. This procedure consists of heating the uncapped tubes in an evacuated oven for several hours. However, one cannot be sure that all moisture has been removed by using this procedure. Hence, a conservative allowance of 10 ppm moisture per pellet is made. The equivalent gas volume at standard conditions has been calculated for each pellet stack. The total volume of gases then at standard conditions is the sum of the three components, that is helium, equivalent gas due to moisture, and the fission gas itself.

Then by knowing the total volume of gas, the gas temperature and the volume of the gas space, the internal pressure in the fuel rod section could be calculated. The internal pressure was calculated by using the following ideal gas equations:

(19) $$\frac{P_1V_1}{T_1} = \frac{P_2V_2}{T_2}$$

(and rearranging terms)

$$P_2 = \frac{P_1V_1T_2}{V_2T_1}$$

Where:

P_1 = atmospheric pressure

V_1 = total volume of gases @ standard conditions

T_1 = standard temperature

P_2 = pressure in gas space

V_2 = volume of fission gas space (hot)

T_2 = average temperature of fission gas space

This pressure is then compared to the allowable pressure which had been determined previously. If the allowable pressure is exceeded by the internal gas pressure, then the entire process must be repeated and a new pellet stack length chosen.

After a pellet stack length and gas space had been established that satisfied all parameters at the worst operating conditions, a graph of radial hot spot factors versus gas space was plotted. Curves of constant power fractions were drawn for the 2.2 per cent enriched quad box fuel rod sections (Figure 17). Only Rod Types I and II were considered since the gas space length at the worst operating condition, for Rod Types III and IV, was small in comparison. Thus, there is no advantage in having modified rod sections in the upper half of the core.

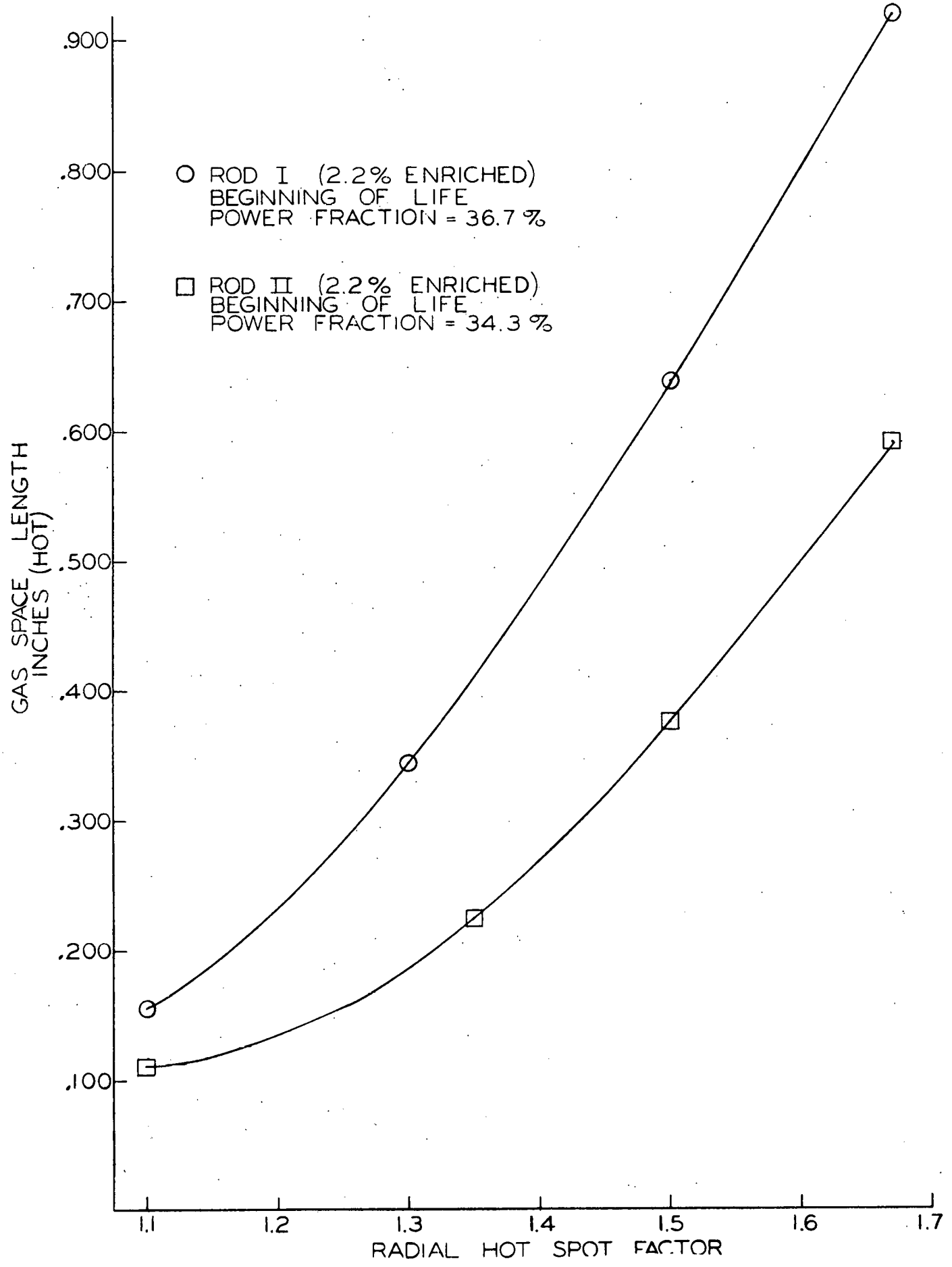

Figure 17...Fission Gas Space vs Hot Spot Factor (43-025-449)

A plan view of the flux profile (radial factors) across Rod Types I and II (2.2 per cent quad box element) was obtained. In this manner the location and required gas space for these rods was determined.

Gas spaces for the 2.2 per cent and 3.2 per cent enriched single box elements were also determined for their respective worst operating conditions. Since the flux profile is almost uniform across the single boxes, all rods in each of the axial quarters are the same. All dimensions for the various fuel rods are shown in Figure 4.

3.2.12 Fuel Rod Assemblies

All of the various types of fuel rod sections are used in the 2.2 per cent enriched quad box element. Seventeen Type I-A's, one Type I-B, and 63 Type I's were required in the lower axial quarter of the typical quad box element. Three Type II-A's and 78 Type II's were required in the middle lower axial quarter. There are 81 Type III's in the middle upper axial quarter. As was mentioned previously, the Type IV-A differs from the Type IV only in the configuration of the upper end cap. Sixteen Type IV-A's are utilized to hold the assembly together.

A typical quad box fuel element is shown in Figure 3. The corner rod and adjacent rods will be positioned in the regions of the highest flux in the quad box. Proper orientation in the quad box is determined by a nickel plug located in the top end fitting. This plug, shown in Figure 3, is located above the inside corner rod. Orientation of the fuel

element within the quad box is shown in Figure 2. This nickel plug also serves as a means of differentiating between the 2.2 per cent enriched single and quad box elements. The 2.2 per cent enriched single box elements do not have the nickel inserts.

The 2.2 per cent enriched single box element is identical in outer appearance to the 2.2 per cent quad box element, except in regard to the aforementioned nickel insert. However, the two lower axial quarters of the single box element are composed solely of fuel rod sections Type I and II.

The 3.2 per cent enriched single box elements have rod section Types I-C and II-C for the lower and lower middle axial quarters, respectively. Axial quarters III and IV will contain the Types III and Types IV and IV-A, respectively. The 3.2 per cent elements will have the upper end fitting chrome plated. This will differentiate between the 2.2 per cent and the 3.2 per cent single box elements.

3.2.13 Column Loads on Supporting Fuel Rods

The total compressive load on the upper fuel bundle is equal to the pre-compression of the nozzle spring plus the product of the pressure drop, end to end, and the area of the bundle, or 440 lb compressive load. The maximum allowable column load on one rod was determined according to the tangent modulus theory[14] using the equation:

$$(20)\quad P_T = \frac{\pi^2 E_T I}{\ell^2} = \frac{A\,\pi^2 E_T}{(\ell/r)^2} = 83 \times 10^{-4}\, E_T$$

$$P_T/A = S_T$$

Where

S_T = stress corresponding to critical load

P_T = critical load

E_T = tangent modulus

ℓ = length = 18.4 in.

r = radius of gyration = 0.338 in.

By use of the curve on Figure 18, P_T was found to be 290 lb by trial and error.

Another type of failure of thin cylindrical shells axially loaded is collapse of the walls. This was investigated using the equation:[15]

$$(21)\quad \bar{P} = \sigma_{yp} \left(\frac{\pi^2}{2\sqrt{3K}} + \pi K \right) t^{1.5}\sqrt{D}$$

Where:

$\bar{P}$ = critical load

σ_{yp} = yield stress = 16,000 psi

t = wall thickness = 0.024 in.

D = mean diameter = 0.337 in.

$k = \dfrac{\pi}{2\left[3(1-\mu^2)\right]^{\frac{1}{4}}} = 1.263$

μ = Poisson's Ratio = 0.45

Which yields

$\bar{P}$ = 213.8 lb for the 0.315 OD rod

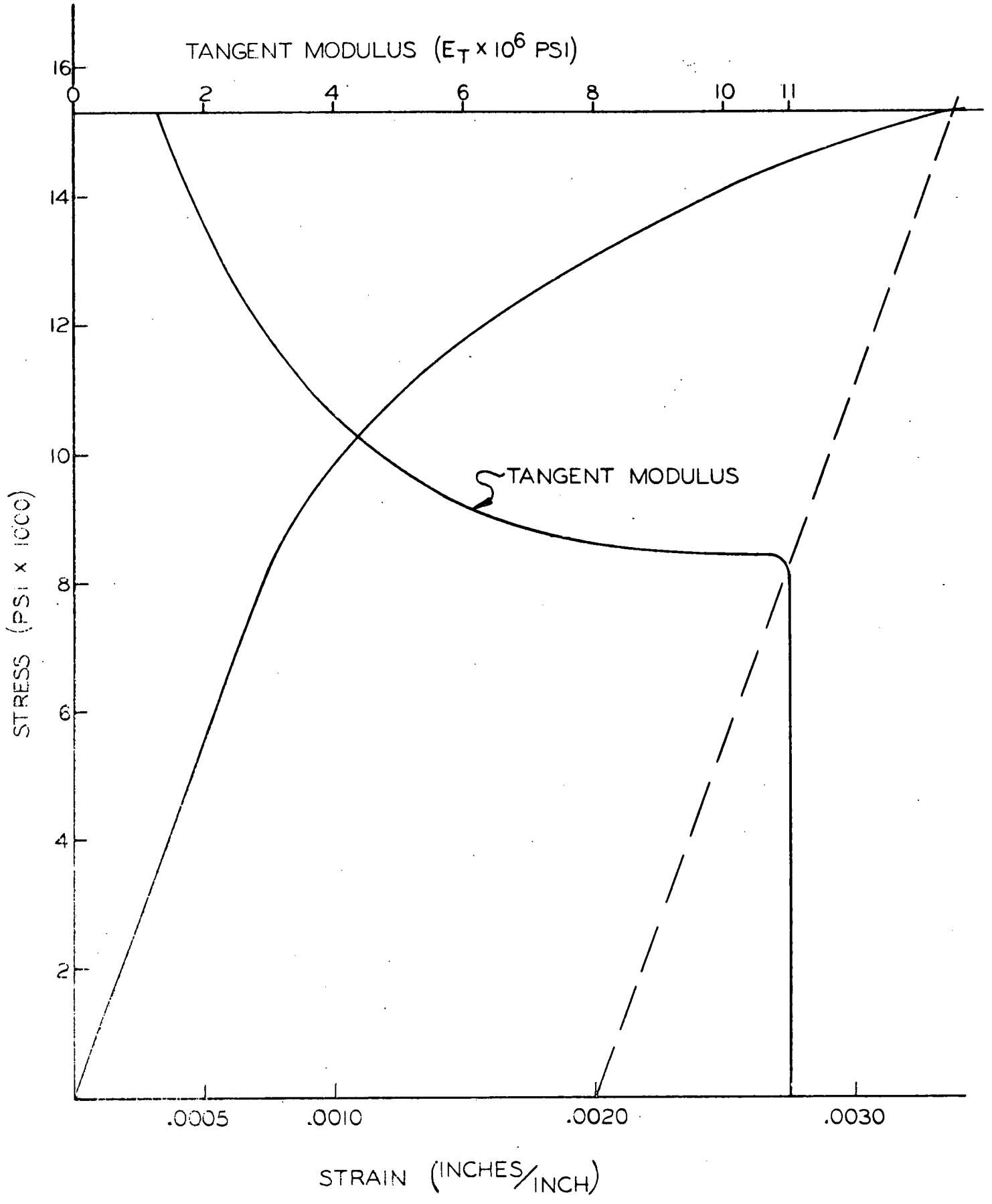

Figure 18...Stress-Strain Curve for Zircaloy-2 Showing Tangent Modulus (43-024-696)

These calculations show that the minimum load which could have any adverse effect on a rod would be 213.8 lb. Since there are sixteen long rods with bolts in the upper fuel rod section, the sixteen fuel rods at these locations will support the compressive load, therefore, the load per rod would be $\frac{440}{16}$ = 27.5 lb, which is substantially less than the allowable load. The compressive load of 440 lb consists of the pre-compression on the spring, the compression of the spring caused by the holddown fixture and the hydraulic forces.

3.2.14 Thermal Bowing of Fuel Rods

The deflection of the fuel rods due to a temperature gradient across the rod diameter was investigated using the equation:[13]

$$(22) \quad \delta_{max} = \frac{\alpha \Delta T L^2}{8d}$$

Where

α = thermal expansion coefficient = 3.4×10^{-6} in/in^{o}F

ΔT = temperature drop across rod diameter

L = rod length between supports

d = rod OD

δ_{max} = maximum deflection

Results of this calculation are plotted on Figure 19. These results show that thermal bowing will not be significant because an impossible heat flux distribution would be required to give sufficient temperature drop across the rod to cause problems.

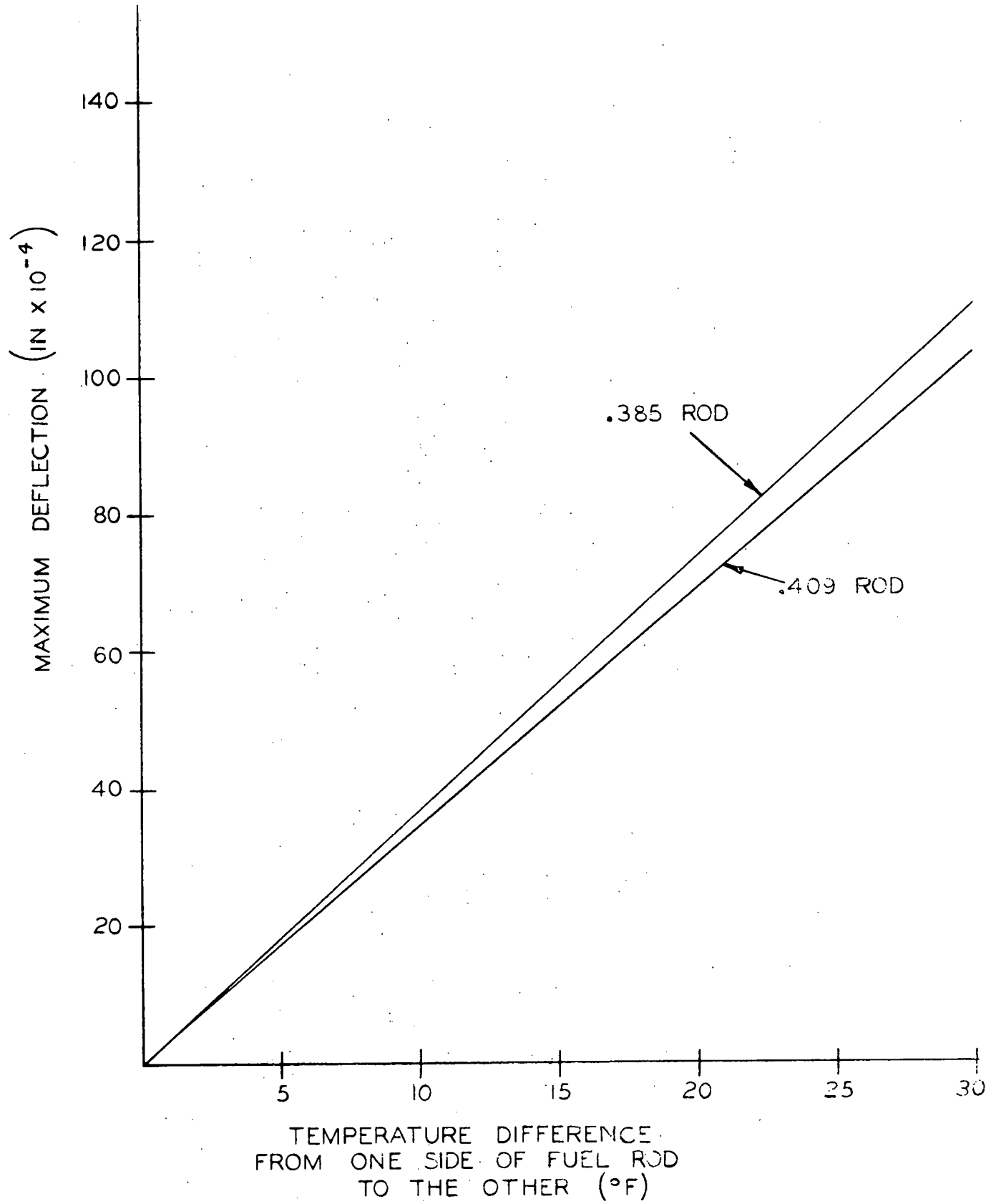

Figure 19...Boiler Fuel Rod Thermal Bowing (43-024-697)

3.2.15 Vibration of Fuel Rods

Natural frequency of fuel rods was plotted as a function of length to assure that the natural frequency of the fuel rods did not coincide with the recirculation pump frequency of 628 cps. The equations used were:

(23) $f_n = 1.57\sqrt{\frac{g\,E\,I}{W\,L^4}}$ for pinned ends

(24) $f_n = 3.56\sqrt{\frac{g\,E\,I}{W\,L^4}}$ fixed ends

Where

f_n = natural frequency

g = 386 in/sec^2

E = Young's Modulus = 10.3×10^6 psi

I = section moment of inertia

W = weight per unit length

L = length

It was assumed that "EI" applied to the rod only and "W" applied to sum of rod plus UO_2. In Figure 20, it can be seen that the natural frequency of the rod is sufficiently removed from pump frequency.

3.2.16 Transients

Some attention must also be given to the startup and shutdown procedures. Since the various reactor parameters are in a constant state of change during startup and shutdown, one must ensure that the internal pressure in the fuel rod sections does not exceed the allowable pressure.

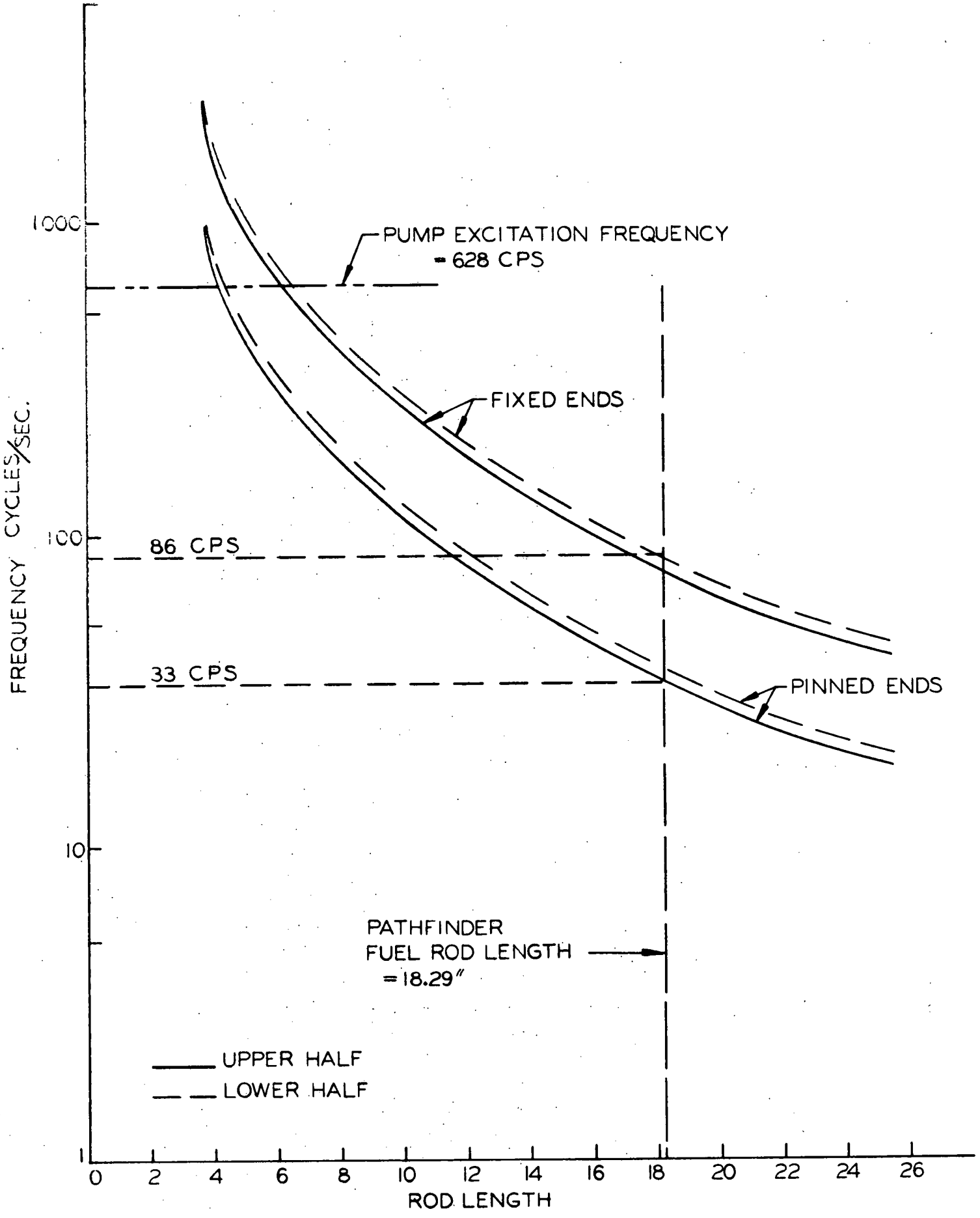

Figure 20...Fuel Rod Vibration Frequencies vs Rod Length (43-024-698)

A plot of the various factors, allowable pressure, internal pressure and system pressure for Rod Section I is shown in Figure 21. The effect on allowable pressure, of the decrease in external pressure, is more pronounced than the increase in allowable stress (lower temperature) at bulk temperatures near the maximum. This accounts for the dip in the allowable pressure curve.

The internal pressure curves (Curves 2 and 3) are conservative since the pressure is assumed to be proportional to the temperature only. In the actual case, the gas space will also increase as the temperature decreases. Then, too, the reactor power decreases more rapidly than pressure, so the temperature is not linear as assumed. The results of this analysis (Figure 21), show that the transient startup and shutdown conditions will not exceed previously established design limits.

3.3 Fuel Element Hardware

3.3.1 Support Grids

Axial support of the fuel rods is provided by support grids, (Figure 22) located at each end of the assembled fuel rods. Stainless bolts project through the support grids and are screwed into the end caps of Rods I and IV-A.

The grid was originally designed to be fastened with retaining rings and a 1000 lb load cell was to be used to limit the lifting capacity of the fuel handling crane. With a minimum of 60 retaining rings in place, the load was distributed over the grid. Stress analysis of a worst possible

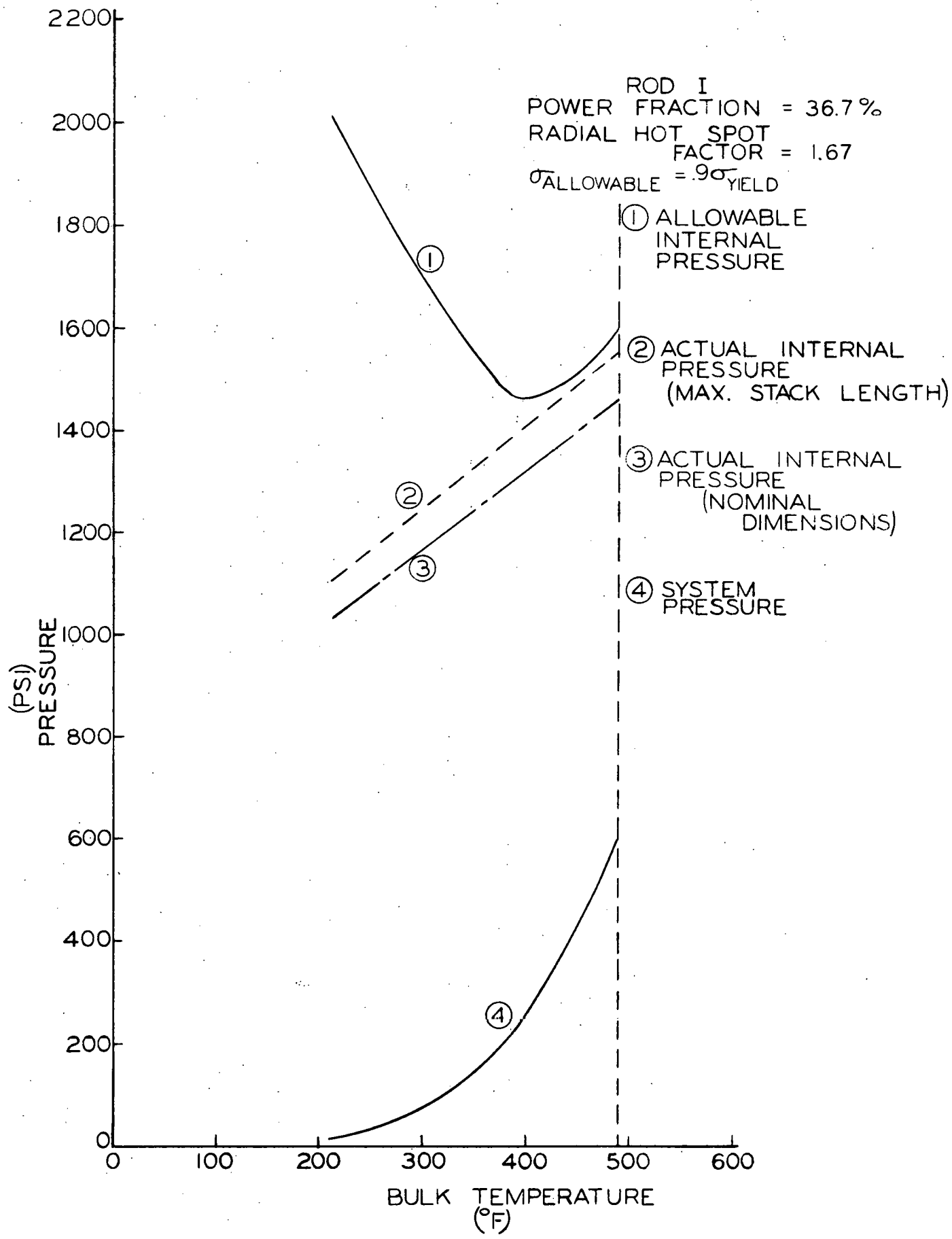

Figure 21...Transient Conditions in Fission Gas Space (43-025-444)

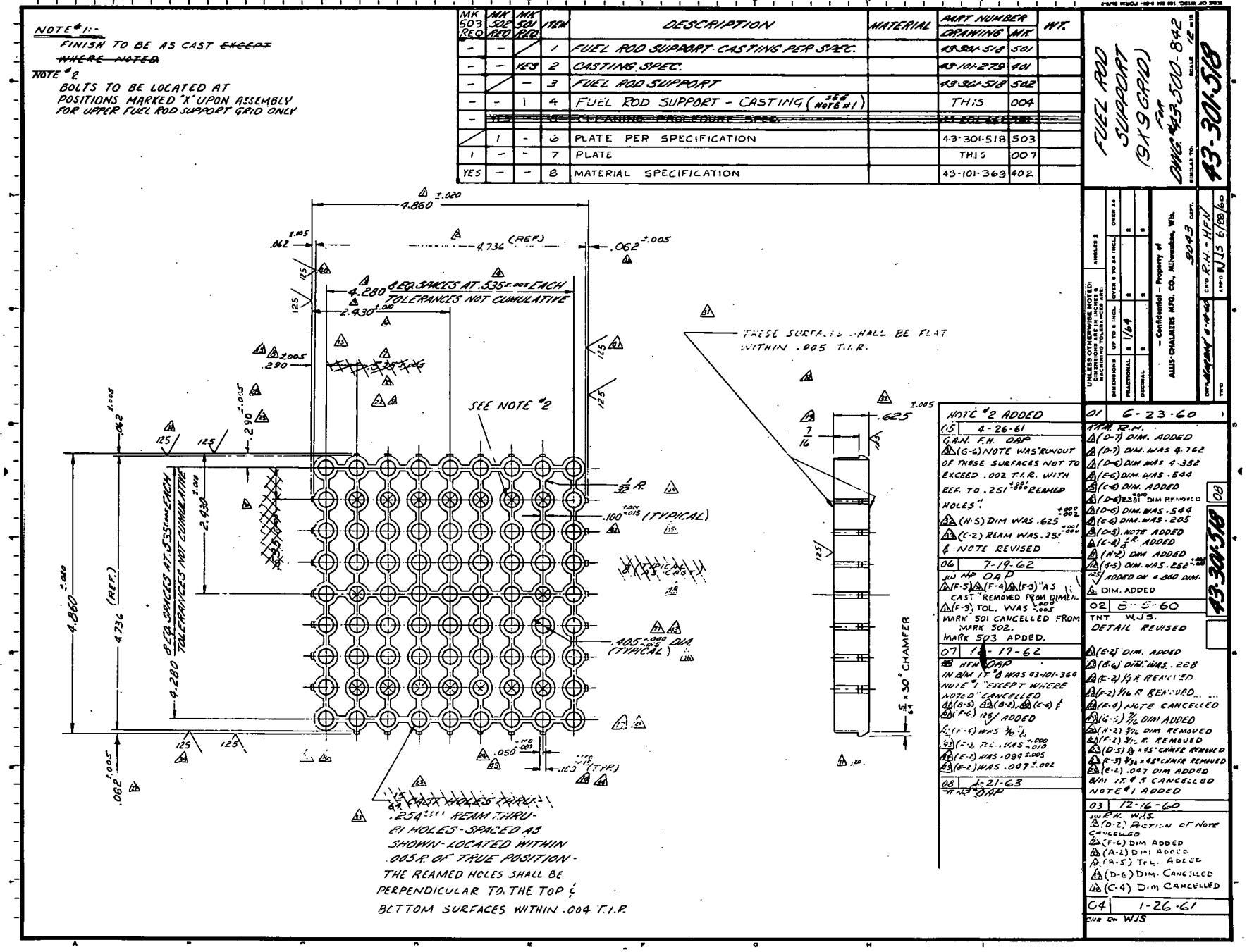

Figure 22...Fuel Rod Support Grid (43-301-518)

case determined the thickness of the grid to be 0.625 in.

After it was decided to use bolts instead of retaining rings, the load was no longer supported by 60 rods with retaining rings but, instead, by some lesser number of bolts. It was desirable not to increase the thickness of the grid in making the change and it was also desirable to increase the limit of lifting from 1000 lb to 2000 lb which is the design capacity of the crane. The criteria for location of the bolts was that the rods having bolts should operate at nearly the same temperature. Since the hot spots occur mainly in the outer row of rods, it was therefore undesirable to put bolts at these locations. The fact that stresses in the grid are higher with loads near the center meant that the best location for the bolts would be in the second row of rods. The grid stresses were analyzed by assuming a total of fourteen bolts located in the second row and considering only one row of the grid itself having a 3/32 in. web. A bending stress of 21,800 psi was calculated for these conditions. Therefore, the grid will not yield under the worst conditions of loading. In assembly of the fuel element, 16 bolts were specified, located as shown in Figure 22.

The fuel element is tied together by means of skirts which are welded to the support grids and screwed to the respective end fittings. For the purpose of welding the skirts to the grid, there are 0.049 in. wide nubs on the outside of the grid. There are 0.050 in. slots in the skirts which match up with these nubs for fusion welding.

3.3.2 Skirts

The skirts consist of a 4 in. wide strip of No. 16 gage 304L stainless steel used to connect the lower and upper end fittings to the fuel rod bundle. They are attached to the fuel support grids and the end fittings as described above. The skirts on the upper end have a 0.042 in. offset to compensate for the difference in size between the upper flange and the upper fuel support grid. Rather than attempt to calculate the stresses in these offset column loaded strips, a prototype was built and tested. This prototype withstood a compressive load of 6000 lb at room temperature without failure or visible buckling. Since the maximum compressive load imposed during operation is only 440 lb @ 500 F, the skirts will not fail in operation.

After the skirts are welded to the support grids, the largest section (across the welds) will fit in a 4.880 in. square envelope and therefore will fit easily in the 4.985 in. minimum box.

3.3.3 Tube Sheets

The fuel element is laterally supported at each joint by a tube sheet. The criteria for design of the tube sheet was that it offered a minimum of axial restraint and a maximum of lateral support to the fuel rods with a minimum decrease in flow area. The rod spacing was determined from physics and heat transfer considerations which required that there be 81 rods on a square pitch, 0.535 in. on center, in a 9 x 9 array. The tube sheet consists of a 23 gauge (0.028 ± 0.002) 304L stainless

sheet which has rings which fit over the studs on the male end caps at the rod joints. The rings are 0.385 OD x 0.251 ID and are joined together for lateral support of the rods by a 0.125 web. It may be noted that the ID of the rings must pass freely over the 0.250 shoulder on the male end cap without being loose. Thus close tolerances are necessary on the tube sheet holes and fuel rod shoulders. A skid is located on each side of the tube sheet. Its purpose is to prevent the fuel rods from rubbing on the sides of the box when the element is being inserted or removed from the core. The skid also serves as a bearing surface through which the fuel element may receive lateral support from the box. The skid consists of a 4 in. x 1/2 in. x 0.050 in. strip of 304 stainless welded to tabs which project from the lattice of the tube sheet. Overall tube sheet dimensions were determined from the box inside dimension (5.000 ± 0.015) and the center-to-center dimension of the outer rods (4.280 ± 0.010). The desirability of having at least a 1/16 clearance between element and box, a 0.004 in. manufacturing tolerance from rod centerline to skid surface and 0.012 in. for differential thermal expansion between tube sheet and box were also considered in determining the tube sheet dimensions.

To prevent the skid from "hanging up" on the box as the element is being lowered into the box, the skid is curved so that its edges touch the rods and only the center acts as a bearing surface. The radius of curvature was determined as shown in Figure 23. The radius of curvature for the skid on the tube sheet between Rods III and IV is calculated in the same manner and equals 0.292 in.

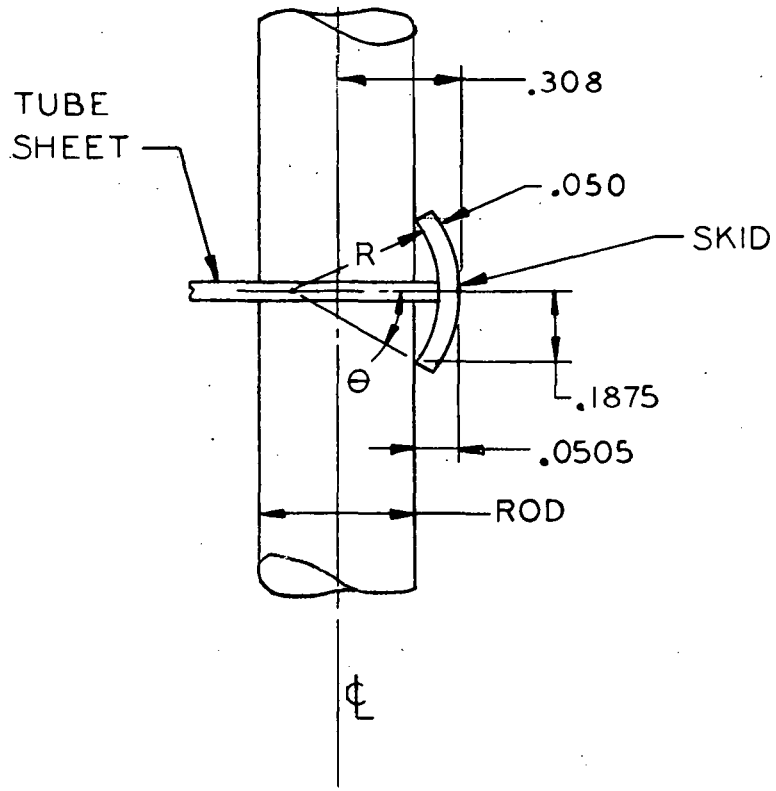

$R \sin \theta = 0.1875$

$R(1-\cos \theta) = 0.0505$

$\cos^2\theta - 1.864 \cos \theta + 0.865 = 0$

$\cos \theta = 0.866$

$\theta = 30^\circ$

R = 0.375" for tube sheet between I and II, and II and III.

Figure 23...Pertinent Dimensions of Skid for Tube Sheet (43-025-882)

3.3.4 Fuel Rod End Caps

The end caps were designed to form a tight joint while passing through the tube sheet. The male end caps of these connections have a 0.250 diameter shoulder which projects through a 0.251 bore in the female end cap. The connection is made with a No. 12 - 28NF Class 2 fit in the threads. The only lateral clearance between the rod and the tube sheet is the 0.001 in. - 0.003 in. diametral clearance between the shoulder and the tube sheet hole. When the fuel rod sections are screwed together, the tube sheet will support the rods laterally and prevent vibrations of the fuel rods at the tube sheet.

There are two kinds of end caps at the ends of the fuel element. In order to understand the reasoning in this design, it is helpful to realize that initially the fuel element was designed using retaining rings in the assembly of the element. These rings were to fit over end cap projections which passed through the support grids. With retaining rings, the differential thermal expansion between the rods was taken care of by 8 bosses 0.061 in. thick on the upper support grid. This meant that only 8 of the 81 rods were restricted in axial expansion while the remainder of the rods had space for 0.061 in. differential thermal expansion.

Due to stress corrosion problems, it was decided that retaining rings should be replaced by bolts which would project through the support grid and screw into a female end cap on the fuel rods. In order to

insure that these bolts won't back off and fall out, the heads are spot welded to the support grids. It is obvious that if all fuel rods were held in place with bolts and all bolts were welded, then this would not allow for differential thermal expansion. For this reason, it was decided that there should be two types of attachment to the support grid at the upper end. At the lower end all 81 rods are bolted. At the upper end, 16 of the rods are bolted and the remaining 65 rods have end caps which project into the support grid. Although there are no bosses on the upper support grid, the axial freedom for differential thermal expansion is gained by having the 65 unbolted rods 0.060 in. shorter than those which are bolted. Fuel rod Section IV-A, at the upper end, has a female end cap at both ends. In order that rods of this type will not be inadvertently switched end for end at assembly, the 0.260 in. bore is omitted on the female end caps receiving the bolts.

3.3.5 Fuel Element Upper End Fitting

The upper end fitting or fuel handling fixture has two primary functions. It centers the fuel element in the box and it receives the fuel handling tool. A quick release device used for handling necessitates a circular entry in the end fitting. Consequently, a round-to-square transition is used, similar to that in the nozzle flange, to assist in a smooth transition from the square flow channel to the round. The 3/8 radius groove shown in the top end fitting of the fuel element, Figure 24, is used to receive the latching elements of the handling tool regardless of tool orientation.

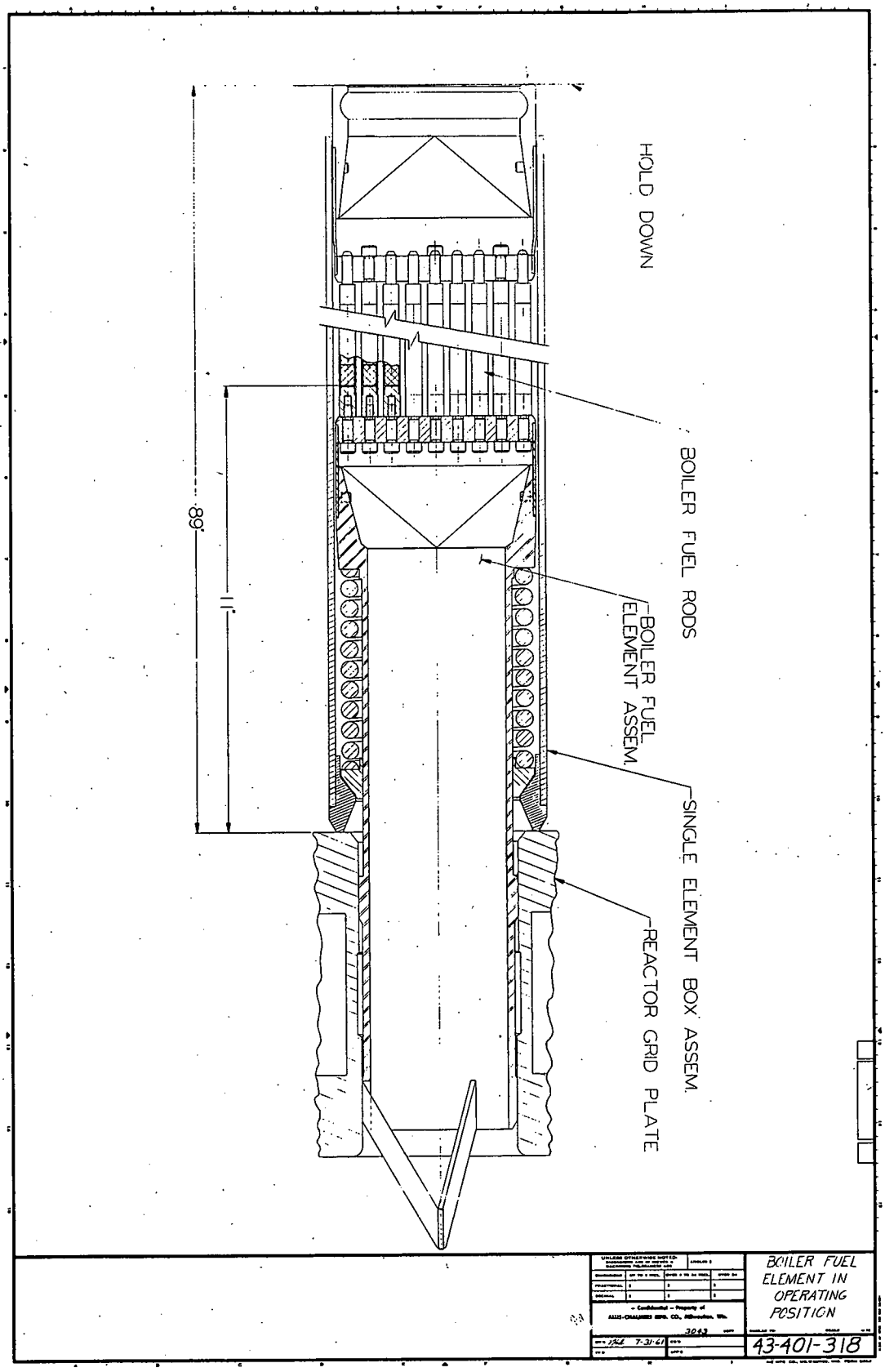

Figure 24...Boiler Fuel Element in Operating Position (43-401-318)

3.3.6 Nozzle Assembly

The lower end fitting or nozzle assembly consists of the nozzle subassembly, ring, spring and nozzle flange as shown in Figure 24. It has the function of directing the flow into the element, positioning the element and supporting it through the ring and spring arrangement.

The lands on the nozzle fit into corresponding lands on a sleeve in the grid plate. The 3.743 $\pm$ 0.001 land moves in a 3.775 $\pm$ 0.001 bore and the 3.878 $\pm$ 0.001 land in a 3.890 bore which means there is a diametral clearance of 0.010 to 0.014 inches. This has been shown through tests to be adequate clearance for nozzle insertion and, at the same time, minimized the leakage.

The entire surface of the nozzle subassembly is chrome plated. Tests have shown that hard chrome plate on Type 304L stainless steel provides adequate protection against galling between the mating lands of the nozzle and grid plate sleeve. Since the ring inner surface can rub on the 3.650 diameter of the nozzle, the chrome plate is added in this portion. Publications indicate that "hard chromium plating of the order of 0.001 to 0.010 in. thick is used for industrial applications where wear is involved."[17] A 0.004 to 0.007 inch thickness was used which proved satisfactory in subsequent nozzle galling tests.

The stresses in the nozzle assembly are confined to the nozzle flange and to the nozzle weld joint.

The maximum load on the nozzle flange to nozzle weld joint is 2000 lb. This is arrived at by assuming the nozzle is frozen in the grid plate sleeve and the fuel handling crane has a maximum lifting capacity of 2000 lb. While this situation is a possibility, it is not expected; i.e., the nozzle should not freeze in the grid. The nozzle weld joint and associated stress diagram are shown in Figure 25.

The following equations can be derived from Figure 25 and are shown in Spotts:[18]

$$(27)\quad \sigma_i = \frac{P}{\text{Throat area}}$$

or

$$(28)\quad \sigma_i = \frac{P}{h \sin 45^\circ \, l} = 2{,}010 \text{ psi}$$

Where

h = leg of weld = .125

P = load = 2000 lb

l = length of circumferential weld = (π) (3.58")

Even if a stress concentration factor of 3 is used, σ_i equals 6030 psi and the weld is adequate. The yield stress for Type 304L stainless steel is 28,000 psi at 100 F.

The spring used in the nozzle assembly was designed with conventional spring design formulas using Inconel "X" as the material.

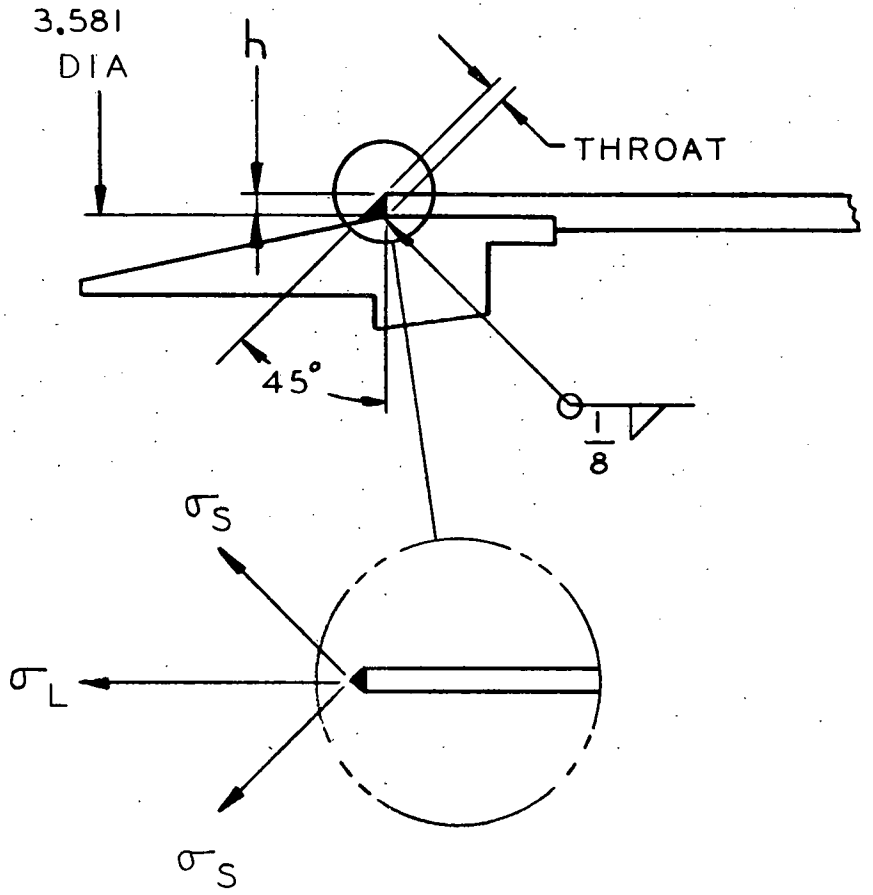

Figure 25...Nozzle Weld Joint and Associated Stress Diagram (43-025-883)

The function of the spring is that of maintaining the fuel element against the holddown grid. In this manner, the fuel element position in the core is fixed axially and at the same time the differential thermal expansion between the element and the boiler shroud is taken up by movement of the nozzle in the grid plate sleeve.

The following assumptions were made:

1. Weight of the element in 100 F water = 227 lb
2. Weight of the element in 500 F water = 233 lb
3. Load due to placement of holddown = 60 lb
4. Total load in 100 F water = 287 lb
5. Total load in 500 F water = 293 lb
6. Torsional modulus (G) of Inconel "X" = 11.25×10^6 at 100 F
7. Torsional modulus (G) of Inconel "X" = 10.5×10^6 at 500 F
8. Maximum allowable stress = 60,000 psi*

*NOTE: This value is 85 per cent of the recommended value of 70,000 psi for Inconel "X" No. 1 temp, cold colled, age-hardened at 500 to 550 F[3] (19)

The wire diameter, d, was established at 0.422 by trial and error. The mean spring diameter, D, is equal to 4.250 in. The dimension was derived by the following equation for spring rate:[20]

$$(29) \quad K_R = \frac{d^4 G}{8 D^3 N}$$

Where:

K_R = Rate #/inch

G = Torsional modulus

D = Mean spring diameter

d = Wire diameter

N = active coils

Assuming 9 active coils, the spring rate was computed to be 64.5 lb/inch. The total deflection in 100 F water is 4.87 in. This includes 0.422 inches which is added to prevent the spring from having an operating height equal to the solid height. The 0.422 inches provides an extra "cushion" of one-wire diameter at the expected operating height.

Other pertinent design data for the spring is given below:

1. Free length = 9.52"
2. Assembled length = 6.833"
3. Load at Assembly = 174 lb
4. Deflection after assembly to support total load = 1.76"
5. Solid height = 4.642"
6. Operating stress = 47,300 psi

At a water temperature of 500 F, the spring rate and operating deflection both change. The spring rate is now 60.2 lb/inch. The operating length increases by the amount of the differential thermal expansion between the stainless boiler shroud and the Zircaloy cladding on the rods. The stainless end fittings are assumed to expand at the same rate as the shroud. The expansion of the stainless end fittings was computed to

be 0.338 inches whereas the Zircaloy-2 expansion was computed to be 0.116 in. This gives an effective differential expansion of 0.222 in.

Therefore at 500 F:

1. Operating spring deflection = 4.23 in.
2. Spring load = 254.5 lb
3. Operating spring stress = 38,400 psi
4. Effective holddown load = 22 lb

Note that when the reactor is at temperature and pressure, there must be coolant flow which would result in additional hydraulic loads to keep the element against the holddown grid.

The variation in spring rate resulting from the tolerances of $\pm$ 0.003 on the wire diameter and $\pm$ 0.032 on the mean diameter was found to be 5 per cent.

This variation affects a corresponding load variation of 14.5 lb at the deflection.

The ground surface of the end coils is chrome plated to prevent crevice corrosion.[21] An added requirement of a hot set at 600 F for 8 hours is expected to minimize the tendency of the spring to relax with time. This requirement, together with the low stress during operation, should yield maximum reliability of spring performance.

The summary of the spring data is as follows:

1.	Wire Size	=	0.422 ± 0.003
2.	Mean Diameter	=	4.250 ± 0.032
3.	Inside Diameter	=	3-53/64 ± 1/32
4.	Active Coils	=	9
5.	Total Coils	=	11
6.	Free Length	=	9-33/64 ± 1/32
7.	Solid Height	=	4.67 Max.
8.	Spring Rate	=	64.5 lb/inch
9.	Ends	=	Squared and Ground

The spring vibration characteristics were analyzed from two different assumptions. First, assuming that the element was not held against the holddown, the frequency of the spring supported mass would be:

$$(30) \quad f_n = \frac{1}{2\pi}\sqrt{\frac{\text{spring constant}}{\text{mass vibrated}}} = 1.65 \text{ cps}$$

Secondly, the natural frequency of the spring itself was calculated from Ricardo's Formula[5]

$$(31) \quad n = 531\sqrt{\frac{r}{w}}$$

Where:

n = vibrations per minute of spring vibrating between its own ends

r = spring rate lb/inch

w = weight of active portion of spring (lb)

and n was found to be 31 cps. These frequencies do not coincide with either the pump-running frequency or impeller frequency. It is also below the expected frequency of the fuel rod sections.

The tapered lead-in at the inlet of the nozzle is added to ease handling during loading. It assists initially in guiding the element

into the box at the top of the core and also helps center the box base plate over the grid plate hole. It is subjected to small loadings, the greatest of which is that of supporting the weight of the fuel element when the fuel element is stood on the snout point. It is structurally adequate.

4.0 TESTS

4.1 Nozzle Galling Test

The lower end of each boiler fuel element is fitted with a nozzle. The nozzle consists of a hollow cylinder with two lands on the outer surface. It projects into a reactor grid plate sleeve made of 304L stainless steel. Due to temperature fluctuations and corresponding thermal expansions, the nozzle will move up and down during reactor operation. Therefore, it is necessary to make the nozzle of a material which will resist galling during this motion when in contact with the 304L grid plate.

In order to select the nozzle material, tests were performed using nozzles of three different materials, 304 stainless, 17-4 pH stainless, and chrome plated 304 stainless. Three chrome plated nozzles were tested having surface finishes of 8, 16, and 20 25×10^{-6} inch rms. All nozzles were used in conjunction with 304 stainless sleeves to simulate the grid plate. Although 304L stainless is used in the reactor, 304 stainless was used in the test due to procurement problems with the 304L. It was felt that this substitution would have no noticeable effect on galling tendencies.

The tests were run in the test apparatus at reactor conditions (489 F, 600 psi). When tested, the 304 and the 17-4 pH stainless nozzles both exhibited a tendency to gall. The chrome plated 304 did not gall, and for the surface finishes of 16×10^{-6} inch rms and better there were only negligible differences in the scratches which were produced in the sleeves.

On the basis of this test, it was recommended that the nozzle should be made of chrome plated 304 stainless steel with a surface finish of 16×10^{-6} inch rms.

4.2 Vibration Flow Test

Two simulated Pathfinder boiler fuel elements were tested in an air-water loop to study their vibrational characteristics under parallel two-phase flow. The rods were lead-filled stainless steel tubes with an outside diameter of 0.375 in. and a wall thickness of 0.020 in. and were fitted with stainless steel end caps. One rod was 36.23 in. long supported at the ends only and the other rod was composed of two sections, each approximately 18.25 in. long, supported at the ends and at the joint between the two sections. Strain gage signals from the vibrating rods were recorded for flow velocities ranging from 15 to 30 fps and for void contents from 0 to 60 per cent.

The tests did not yield data which could be used to correlate and to predict the precise vibrational behavior of any similar rod under parallel single or two-phase flow. However, the following conclusions can be made about the vibrations of rods experiencing parallel two-phase flow.

1. The rods will vibrate at their natural frequency. The damping effect due to the fluid is not sufficient to cause measurable change in frequency.
2. Vibration amplitudes are a function of the fluid turbulence. Consequently, the spacer arrangement, gas-liquid ratios and other variables have an effect that make analytical solutions impossible.

3. The dominant variable affecting vibration amplitudes appears to be the gas-liquid ratio.

4. Vibration of the Pathfinder boiler rods will not be excessive. It is expected that the amplitudes will be of the order of 0.005 in. maximum with a frequency range of 33 to 86 cps. The distance between the tube sheet spacers on the fuel element was finalized as a result of the information gained in this test.

5.0 PROTOTYPE

A prototype of the fuel element assembly was fabricated substituting solid stainless steel rods for the Zircaloy clad fuel rods and a stainless steel spring for the Inconel "X" spring. The prototype was built for the following reasons:

1. To give a feel for the rigidity of the assembly,
2. To reveal assembly difficulties, if any,
3. To demonstrate the ability of assembly with the tolerances specified, and
4. To assist in the development of specification and drawings with respect to dimensional inspection such as twist and bow of the assembly.

The assembly that was built proved somewhat disappointing due to the fact that many of the tolerances were not met. Specifically, the tolerance on the 1/4 in. holes in the fuel rod grid supports were not held. The overall dimension on the tube sheets was exceeded also. Because of this, the behavior of the element in the box with flow could not be studied; i.e., the fit between the flow test box and the prototype tube sheets skids is not representative of the expected fit in the reactor.

In spite of these items, however, the prototype proved useful because:

1. It clearly demonstrated the need for inspection of the assembly in the vertical position. The assembly is not rigid enough to

allow inspection for straightness and twist on a surface plate. Consequently, the assembly drawing calls for inspection by vertical insertion into an inspection fixture without attendant damage to the fuel element.

2. Because the tube sheets fit tightly into the flow test box and the element was inserted and withdrawn from the box without damage to the tube sheets or skids, confidence in the tube sheet design was established.
3. Upon disassembly and assembly, the requirements for a fuel-rod-to-fuel-rod tightening specification became apparent.
4. In spite of the fact that the tube sheets are not "flat" when the assembly is completed (being deformed due to the tolerance buildup on the rods) it has sufficient strength to provide necessary lateral support of the fuel rods.

REFERENCES

1. Roberts, D. R., "Thermal Expansion of UO_2 Pellets," Unpublished 4/18/60.

2. Seely and Smith, Advanced Mechanics of Materials, 2nd Edition, p. 301.

3. Sturm, R. G., "A Study of the Collapsing Pressure of Thin-Walled Cylinders," University of Illinois Engineering Experiment Station Bulletin Series #329.

4. Etherington, H. Nuclear Engineering Handbook, p. 1.61.

5. Ibid

6. Ibid

7. Seely and Smith, Op. Cit., p. 299.

8. Bezella, W. A., Teeter, C. L., and Hill, L. D., "Gaseous Release Evaluation Routine," ACNP-6116.

9. Booth, A. H., "A Method for Calculating the Diffusion of Radioactive Rare Gas Fission Products from UO_2 Fuel Elements," AECL Chalk River Report DCI-27.

10. Eichenberg, et al, "Effects of Irradiation on Bulk UO_2 WAPD-183 (1957).

11. Bilodeau, G. G., et al, "An IBM-704 Code to Solve the Two-Dimensional Few Group Neutron-Diffusion Equations," WAPD-TM-70, August 1957.

12. Sherman and Sherba, "PWR Reference Fuel Rod Design," WAPD-RDA-71, p. 13.

13. Halden, F. A., et al, "Thermal Expansion of Uranium Dioxide," TID-5722.

14. Seely and Smith, Op. Cit., p. 595-606.

15. Alexander, J. M., "An Approximate Analysis of the Collapse of Thin Cylindrical Shells Under Axial Loading," The Quarterly Journal of Mechanics and Applied Mathematics, Clarendon Press, Volume XIII, Part 1, February, 1960, pgs. 10-15.

16. Vlies, L. E., "Thermal Bowing of Rods," 11/3/60, Unpublished.

17. Clark & Varney, Physical Metallurgy, pp. 214.

18. Spotts, Design of Machine Elements, pp. 224-227.

19. Inco Bulletin T-35 page 40.

20. "Handbook of Mechanical Spring Design," Associated Spring Corp. p.24.

21. Corrosion and Wear Handbook.